We thank the reviewer for the helpful comments which improved the manuscript significantly. The detailed replies on the reviewer's comments are given below and structured as follows. Reviewer comments have bold letters, are labeled, and listed always in the beginning of each answer followed by the author's comments including (if necessary) revised parts of the paper. The revised parts of the paper are written in quotation marks and italic letters.

Comments:

1. **Lines 46-60. A very incoherent paragraph. Cloud inhomogeneity effects on gridded fluxes are mixed with effects on satellite retrievals. Lines 49-50 talk about retrievals, and the next sentence talks about GCMs. Moreover, the first problem facing GCMs is not the lack horizontal photon transport, but the absence of subgrid variability, i.e., the unavailability of PDFs of cloud condensate for each layer. If such PDFs were available at least IPA calculations would in principle be possible (still no horizontal transport). The dissemination of confusion continues later on. In lines 55-58 the limitations of IPA compared to 3D are followed in lines 58-60 by an irrelevant example of errors found by Shonk and Hogan when comparing PPH and IPA.**

We agree on that. Especially, the reference to GCMs were confusing and we agree that the reference to Shonk and Hogan (2008) is irrelevant and confusing at this point. Therefore, we removed it and revised the paragraph as follows:

"Several independent studies investigated the influence of the plane-parallel assumption on cloud retrievals (e.g. Cahalan, 1994; Loeb and Davies, 1996; Marshak et al., 1998; Zinner et al., 2006; Varnai and Marshak, 2007). They found that the magnitudes of model biases are related to the degree of horizontal photon transport. In 1D radiative transfer simulations clouds are divided into separate vertical columns with horizontal homogeneous optical and microphysical properties (independent pixel approximation, IPA). However, horizontal photon transport cannot be neglected in case of inhomogeneous clouds. Additionally, multiple scattering due to 3D microphysical cloud structures smooth the horizontal radiation field. On small scales, this limits the accuracy of IPA. For example, Cahalan (1994) and Marshak et al. (1995) revealed discrepancies for individual pixel radiances exceeding 50 % due to a plan-parallel bias."

"In many remote-sensing applications clouds are assumed as plane-parallel (Francis et al., 1998; Iwabuchi and Hayasaka, 2002; Garrett et al., 2003), which may introduce biases into the modeled radiation budget (Shonk et al., 2011). For example, in the cases of cirrus, Carlin et al. (2002) found a plane-parallel cirrus albedo bias of up to 25 % due to spatial cirrus inhomogeneity. For Arctic stratus over variable sea-ice surfaces, Rozwadowska and Cahalan (2002) reported a plane-parallel albedo bias of less than 2 %, but an absolute value of the transmittance bias that can exceed 10 %."

2. Lines 61-68. Here, cloud overlap is mixed into 3D effects and Monte Carlo discussion. Misleading. You can account for overlap perfectly, but still ignore 3D effects by performing IPA calculations on the perfectly overlapped cloud field.

The reviewer is right. Talking about cloud overlap schemes at this point is misleading. Therefore, we removed those parts, which are related to cloud overlap schemes, in the resubmitted version of the manuscript.

3. Lines 75-77. I'm sure that ECMWF models do not need the two point statistics of cloud structure (as derived by autocorrelation and power spectrum analysis), but some information on the PDF, i.e., the inhomogeneity parameters of section 3 derived from one point statistics, so invoking "spatial features" "below the meter scale" is again inappropriate.

In conjunction with the comment above and comments by the other reviewers we removed the reference to ECMWF models in the resubmitted version of the manuscript. We further revised the statement "spatial features below the meter scale" to clarify that this is related to clouds in reality.

"General circulation or numerical weather forecast models require sub-grid scale parameterizations of, e.g., cloud structures, liquid water content (LWC), and/or ice water content (IWC) (Huang and Liu, 2014). In reality, cloud structures reveal spatial features down to distances below the meter scale (Pinsky and Khain, 2003). Therefore, measurements with appropriate spatial and temporal resolution have to be conducted in order to derive the needed parameterizations. […]"

4. Lines 141-142: "However, rho_tau can exceed values of unity and depends on the average value might lead to misinterpretations." Why? I don't see anything wrong with values greater than unity.

That is true. There is nothing wrong with values greater than unity. This wording belonged to a former version of the manuscript, where we wanted to say that there is no upper limit for ρ_τ where the clouds can be found to be inhomogeneous to 100 %. We revised this part by the following:

"However, ρ_τ has no predefined upper limit, which might lead to misinterpretations in a variability analysis. This renders ρ_τ not as a quantitative, but qualitative measure only."

5. Lines 157-158: It would be simpler to say that chi is the scaling factor with which mean tau needs to be multiplied to approximate the IPA albedo.

We have used the suggested wording from the reviewer to simplify this sentence.

"Thus, the logarithmically averaged τ provides a way to account for cloud inhomogeneity effects in plane-parallel radiative transfer calculations using χ_τ as a scaling factor with which τ needs to be multiplied to approximate the IPA albedo."

6. **Page 7: One has to be careful when comparing inhomogeneity parameters across publications. First, pixel size matters. Second, and most importantly, the domain size matters. The bigger your reference domain, the wider the PDF, the larger the inhomogeneity. So this is by no means a trivial comparison.**

We thank the reviewer for this advice. Indeed, a comparison of the results is complicated for different pixel and domain sizes. However, we still like to show and refer the results from other studies. Therefore, we kept this comparison, but we included a paragraph, which points out the restriction of a comparison. The reader has to keep in mind that the results from the different studies are related to different pixel and domain sizes. Furthermore, we included the pixel and domain size of the investigated cases in Table 1 and added the pixel and domain sizes for the literature cases at the relevant parts.

"The three 1D inhomogeneity parameters ρ_τ, S_τ, and χ_τ are calculated for each retrieved field of τ_{ci} and τ_{st} from the CARRIBA and VERDI campaigns. The results are listed in the right three columns of Tab. 1. When comparing them to literature values one has to keep in mind that cloud inhomogeneities appear on different spatial scales. E.g., cloud fields may change on synoptic scales (~ 100 km) or dynamic scales (10 – 100 m) depending on the cloud type. Therefore, inhomogeneity parameters depend on the pixel and domain size of the analyzed cloud fields. The larger the domain size or the smaller the pixel size is, the broader the probably density function of the cloud parameter may become. Therefore, a comparison of different cloud cases is only valid when pixel size and cloud domain are in the same range."

We also revised this statement in the conclusion part of the manuscript:

"Considering the pixel and domain size of the analyzed measurements, the results from the calculated 1D inhomogeneity parameters ρ_τ, S_τ, are in agreement with values given in the literature for similar cloud types."

7. **Lines 188-190. It's not a matter of directional dependence only. It's mostly a matter of spatial coherence of cloud condensate, in other words how the variability is distributed across scales.**

That is true. Therefore, we have included this statement to the relevant sentence.

"Therefore, not only the horizontal inhomogeneity, but also the spatial coherence of cloud inhomogeneity parameters and their directional dependence need to be investigated (Hill et al., 2012)."

8. **Lines 204-205: Why are negative autocorrelations ambiguous?**

The reviewer is right. The use of the word "ambiguous" is not suitable for the statement we wanted to give here. We revised the paragraph by the following lines to clarify what we wanted to say at this point:

"Here, only the degree of correlation matters; the positive or negative sign of the autocorrelation result is of less importance. To avoid misinterpretations with the sign, the squared autocorrelation function $P^2_\tau(L_x, L_y)$ is used here.

9. Eq. (5): If the scale length is typically defined as the distance at which the autocorrelation drops to 1/e, shouldn't the scale length of squared autocorrelation be defined as the distance where it drops to 1/eˆ2?

We thank the reviewer for this advice. It is true that $1/e^2$ should be used as a threshold when the squared autocorrelation function is used. We recalculated the decorrelation lengths, revised the relevant figures, tables, and text parts. However, the overall conclusion we made on behalf of the decorrelation lengths has not changed. Only the magnitude of the derived values for the decorrelation lengths have changed. Therefore, here in this reply, we only like to show the revised Figure 4. The remaining changes to the manuscript with regard to new decorrelation length values are marked in the additionally submitted author's response document.
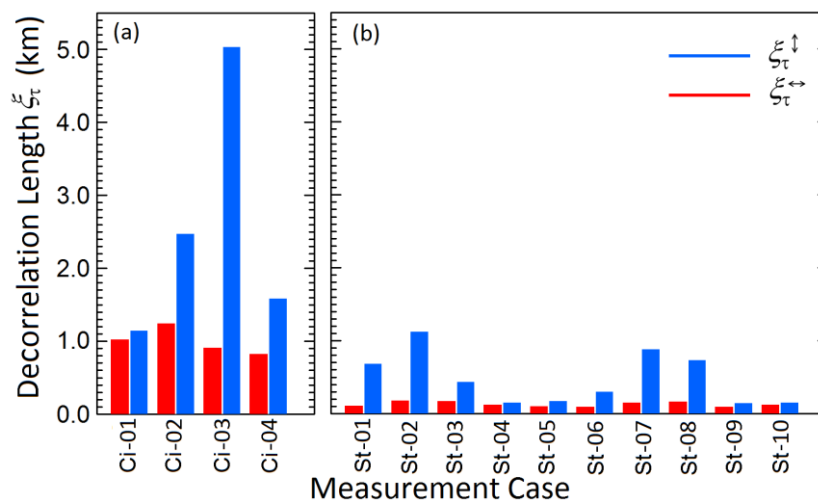

Fig. 1: Revised Fig. 4 using the new threshold for calculating the decorrelation length.

10. Lines 255-256: It's not that they are not well-suited, it's that by themselves they provide incomplete information, i.e., not the whole story.

We revised this sentence by the reviewer's suggestion.

"This reveals that the 1D inhomogeneity parameters ρ_τ, $S\tau$, and χ_τ just provide incomplete information for a comparison of different types of clouds as they are not able to consider the horizontal structure of cloud inhomogeneities."

11. Power spectrum scale break analysis: Have the authors given any thought on whether the comparisons of scales in terms of physical units (m) makes sense when the pixel sizes are different? With pixel size varying, the extent to which the smoothing is resolved is also different, so I was wondering whether defining the scale lengths in terms of pixel number would bring the results closer together.

Yes, we had a thought on this. It is right, a comparison of scales in terms of physical units (m) may be difficult, when the pixel sizes are different. However, here in this case they differ not much. Indeed, along the swath (pixel width) the pixel size for the subtropical cirrus cases is twice as large as for the Arctic stratus cases. This is due to the geometry and different

distances between sensor and cloud. However, the pixel size across the swath direction (pixel length), which depends on the integration time, cloud/ aircraft velocity, is almost the same for the measurements during CARRIBA subtropical cirrus) and VERDI (Arctic stratus). The pixel length is about 5±2 m for both cases. Furthermore, the differences are far below the detected scale breaks. Therefore, a comparison is possible in this case. To better clarify this issue, we added the following lines to the manuscript:

"[…] Furthermore, both cloud cases, subtropical cirrus and Arctic stratus, exhibit a similar pixel length along L_y (5±2 m), which results from the chosen frame rate (subtropical cirrus: 4 Hz, Arctic stratus: 30 Hz) and given cloud (20 m s^{-1}) and aircraft velocity (70 m s^{-1}). This allows a direct comparison between these two different cloud types with different observation geometry."

<u>Typos and other minor stuff:</u>

1. **Line 10: "VERtical" instead of "VERical". Also Line 97.**

Changed to *"VERTical"*

2. **Lines 120 and 272: I think you wanted to use "fingerprint' rather than "footprint". The term "footprint" in remote sensing indicates the resolution, i.e., pixel size.**

Changed to *"fingerprint"*

3. **Line 328: "inhomogeneity".**

Changed to *„inhomogeneity"*

4. **Line 337: "too small".**

Changed to *"too small"*

We thank the reviewer for helpful comments which improved the manuscript significantly. Especially, by adding more explanations the revised manuscript will be easier to understand for the reader. The detailed replies on the reviewers comments are given below and structured as follows. Reviewer comments have bold letters, are labeled, and listed always in the beginning of each answer followed by the author's comments including (if necessary) revised parts of the paper. The revised parts of the paper are written in quotation marks and italic letters.

1. **However, in addition to the comments and suggestions listed below, my main concern with the paper is the lack of a clear statement on what new we were supposed to learn at each step of both (the one-point and the two-points) analyses provided in the paper. What is the main message the authors want us to take home after reading it? I got a feeling that the paper is much more descriptive than conclusive. I'd like to see a list of bullets/statements, at least, in the 'Summary and Conclusion' section.**

The reviewer is right. So far we had been too focused on the feasibility of the study and missed to point out the conclusions of our analysis clearly. We did not use a list of bullets, but we revised the conclusion part to make the most important results more clear.

"[…] Furthermore, the results from the 2D analysis showed that for the observed cloud cases the subtropical cirrus was more homogeneous than the Arctic stratus. This result was not available from the investigation of the commonly used 1D inhomogeneity parameters. Therefore, using 2D methods in future studies for the characterization of cloud inhomogeneities is advisable, since their information content exceeds the information content of the commonly used 1D inhomogeneity parameters. Nowadays, 2D images of cloud fields are widespread by e.g., measurements of all-sky cameras or satellite observation with high spatial resolution. Applying the presented methods to such continuous measurements would provide detailed views into the climatology of cloud inhomogeneities. […]"

"[…] We found such differences for more than the half of the observed cloud scenes. Therefore, the directional structure of cloud inhomogeneities should be taken into account, when cloud inhomogeneities are characterized. Clearly some clouds will have less directional dependence of cloud inhomogeneity, but this does not mean it is not useful to measure it. It is expected that the information content derived from the directional analysis of cloud inhomogeneities can clearly improve sub-grid scale parametrizations in weather and climate models. For this, depending on the application, the decorrelation length (size and structure of cloud inhomogeneities) or the scale breaks (horizontal photon transport, 3D radiative effects) may provide better proxies compared to commonly used 1D inhomogeneity parameters.

However, so far only two cloud types were investigated. To build up a better idea on cloud inhomogeneity of different cloud types, more high definition observations of cloud fields are needed. Beside dedicated field campaigns, continuous observations by all-sky cameras or satellites with high spatial resolution such as LandSat (15-90 m resolution) or ASTER (Advanced Spaceborne Thermal Emission and Reflection Radiometer, 15-90 m resolution) may provide the required data.

The 1D and 2D autocorrelation functions and Fourier analysis in conjunction with the derived decorrelation length and scale breaks are a helpful tool to verify cloud resolving models in terms of typical horizontal cloud geometries."

2. **A) The list of references is very rich but, as always, is incomplete. I would definitely add two more very relevant papers. The first one is**

   Davis, A., Marshak, A., Gerber, H., and Wiscombe, W., 1999: Horizontal structure of marine boundary-layer clouds from cm– to km–scales. J. Geophys. Res. 104, 6123-6144.

   In this paper the authors discuss the structure of marine stratocumulus clouds down to 4-cm scale using both spectral and structure function analyses.

We added the reference at the point where we are talking about the small-scale break. Please check comment number 3 for our changes .

   B) Another paper is

   Barker, H.W., B. A.Wielicki, and L. Parker, 1996: A parameterization for computing grid-averaged solar fluxes for inhomogeneous marine boundary layer clouds. Part II: Validation using satellite data. J. Atmos. Sci., 53, 2304–2316.

   (May be also the Part 1). This paper, I believe, was the first to use the ratio $v=(<\tau>/\sigma\tau)2$ to quantify cloud inhomogeneity.

We have also included a reference to this paper in the current manuscript

"Therefore, similarly to the studies by Barker et al. (1996), who used ratios between mean τ and the variance of τ, Davis et al. (1999) and Szczap et al. (2000) utilized the normalized inhomogeneity measure ρ_τ to quantify the horizontal inhomogeneity of τ."

3. **Small-scale break $\xi_{\tau,S}$. I wonder if the small-scale noise can be reduced by averaging over all cases or over all columns (or rows) in one case. Also, please, compare the location of your small-scale breaks with the once reported by Davis et al. (1999). It was not clear for me what could be learned about cloud structure from the reported small-scale breaks. How does your conclusion depend on pixel size and uncertainty in observations? Please summarize.**

If we average over all columns as proposed by the reviewer the result looks like in Fig. 6 from the original submitted manuscript. The overall appearance of the lines is more smooth then, but their distribution on the y-direction is relatively broad. Therefore, we decided to use the power spectral densities along and across the prevailing direction only for the discussion of the small-scale break. We have also compared the results to the values given by Davis et al. (1999), from which it becomes clear that the small-scale break may have a physical explanation (for scales larger than the pixel size) and is not only related to the white noise, which of course is the reason for the flat power spectral signal for scales below the pixel size. However, since there is a directional behavior we like to keep this paragraph, although it is not possible to fully explain the reason for the small-scale breaks, which are in larger size ranges than the pixel size.

"[…] Furthermore, the ranges of the derived small-scale breaks $\xi_{\tau,S}$ are found to be close to the ranges of the small-scale breaks reported in literature. Davis et al. (1999) derived small-scale breaks for a broken-stratocumulus/towering cumulus cloud complex from LWC measurements with a particulate volume monitor probe (4 cm resolution) at ranges of about 2-5 m. They proposed that those small-scale breaks are related to extreme values in the detected LWC, which appear on small horizontal scales. Besides Poissonian fluctuations of the cloud optical thickness τ and the white noise related to power spectral signals at scales below the pixel size this might be a further explanation for the derived small-scale breaks in the current study and needs to be investigated in further studies."

4. **A) Large-scale break ξτ,L. After Fig. 7, I'd recommend to mention that CARRIBA ξτ,L << VERDI ξτ,L especially, for the most homogeneous cases of C-02 and C-03. This is partly because ξτ,L, as the radiative smoothing scale, is the harmonic mean of the cloud geometrical thickness and the transport mean free path. Both factors are much smaller for Arctic stratus than for cirrus.**

We thank the reviewer for this advice. We used the reviewer's suggestion and included this information at the end of the relevant paragraph.

"[…] Furthermore, the resulting large scale breaks $\xi_{\tau,L}$ confirm the results from the derived decorrelation lengths ξ_{τ} that the subtropical cirrus observed during CARRIBA is more homogeneous (larger ξ_{τ} and $\xi_{\tau,L}$) than the Arctic stratus from VERDI (smaller ξ_{τ} and $\xi_{\tau,L}$). This is related to the fact that $\xi_{\tau,L}$, which is the radiative smoothing scale, is a function of the cloud geometrical thickness and the transport mean free path. For Arctic stratus both parameters are significantly smaller than for subtropical cirrus."

B) I'd also recommend comparing the theoretical values of the radiative smoothing scale with the observed ones, ξτ,L.

We have now included a comparison to theoretical values reported by Marshak et al. (1995):

"[…] Especially the values for the Arctic stratus are in the size range, which was also reported by Marshak et al. (1995), who found scale breaks for fractal clouds in the range of 200-500 m. […]"

5. **A) Retrieval of τ. I know that several references on the retrieval processes are given. However, the way τ-field has been retrieved is important for understanding the analysis provided in the paper. The main question is how much the retrieved τ-field is influenced by 3D radiative effects. I'd recommend to briefly describing here the retrieval processes.**

We have now included the most necessary information on the retrieval technique we applied in this study:

"Simulations are performed with the radiative transfer solver DISORT 2 (Discrete Ordinate Radiative Transfer). Input parameters such as cloud optical properties, aerosol content and spectral surface albedo are provided by the library for radiative transfer calculations (libRadtran, Mayer et al., 2005). The required profiles of thermodynamic parameters are derived from measurements from radiosondes and/or dropsondes. Despite of assuming plane-parallel clouds in the simulations, the investigation of 3D radiative effects is still possible using the retrieved fields of τ, but directional features related to the scattering phase function are avoided. $I_\lambda^\downarrow$ and $I_\lambda^\uparrow$ were simulated as a function of values of τ_{ci} and τ_{st}, respectively. The simulations were performed for all scattering angles within the FOV of AisaEAGLE. Thus, simulated grids of possible $I_\lambda^\downarrow$ and $I_\lambda^\uparrow$ and corresponding τ_{ci} and τ_{st} are available for each time step of the measurements and each spatial pixel. The retrieved τ_{ci} and τ_{st} are derived by interpolating the simulated $I_\lambda^\downarrow$ and $I_\lambda^\uparrow$ to the measured value for each spatial pixel using a linear interpolation. More detailed descriptions and sensitivity tests of the applied retrieval procedures are reported by Schäfer et al. (2013) for subtropical cirrus and by Bierwirth et al. (2013) as well as Schäfer et al. (2015) for Arctic stratus. […]"

B) Another point, I was not convinced that from analyzing the structure of the retrieved cloud optical depth fields for inhomogeneity, one can learn something new compared to the analysis of the measured fields of radiance. I'd recommend, in parallel to, say, Figs. 5 or 6 (or even 7), showing some results of the analysis of energy spectra for the radiance fields.

There is one major reason for using cloud optical thickness fields instead of radiance fields in this study. If radiance fields are used instead of cloud optical thickness, the features of the scattering phase function would contaminate the analysis of cloud inhomogeneity structures performed with 2D methods. For one-dimensional analysis using autocorrelation functions or Fourier transformations cloud parcels are observed within the same narrow scattering angle range. Changes in the observed radiance field are then most probably related to the cloud and not to the features of the scattering phase function. However, for 2D images this is different since they cover a wide range of scattering angles. Please find below in Fig. 2 a measurement example extracted from Schäfer et al. (2013), which shows a measured radiance field (left) and the corresponding cloud optical thickness field (right). The radiance plot clearly shows features of the scattering phase function, namely the increase of radiance closer to the Sun (located on the right side of the image). This signature of the radiance field would be imprinted into the autocorrelation or Fourier analysis. In other measurement cases e. g. also halo events or cloud bows could be imprinted in the radiance field. Therefore, we have used the corresponding fields of cloud optical thickness, where those features of the scattering phase function are not included as can be seen in the image on the right side.
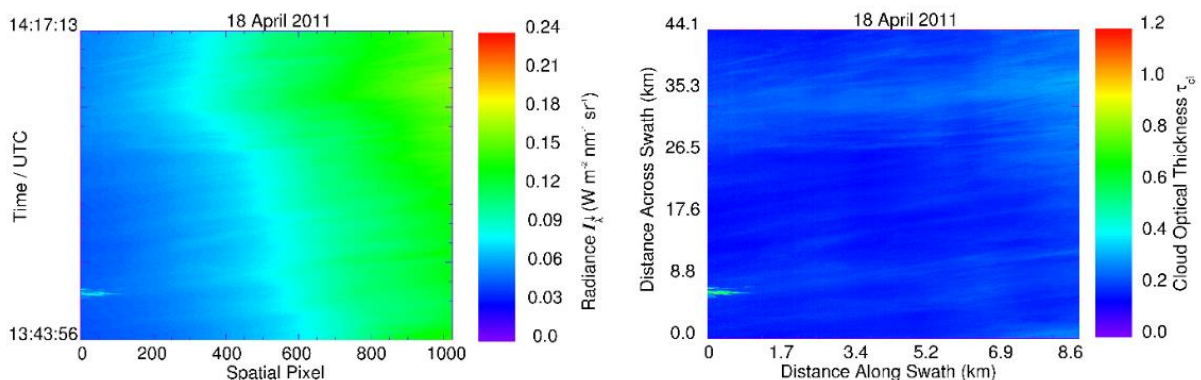

Fig. 2: Radiance field (left) and corresponding cloud optical thickness field (right) (Schäfer et al., 2013)

We have also included more information and extended the relevant paragraph to make it more understandable to the reader.

"As proposed by Marshak et al. (1995), Oreopoulos et al. (2000), or Schröder (2004), horizontal cloud inhomogeneities are studied by scale analysis of cloud-top reflectances. However, radiance measurements include the information of the scattering phase function (e.g., forward/backward scattering peak, halo features) in the measured fields of radiance (Schäfer et al., 2013). To avoid artefacts in the scale analysis resulting from such features, parameters that are independent on the directional scattering of the cloud particles have to be analyzed. The cloud optical thickness τ does not include the fingerprint of the scattering phase function. Therefore, the ground-based and airborne measured fields of $I^{\downarrow}_{\lambda}$ (CARRIBA) and $I^{\uparrow}_{\lambda}$ (VERDI) were used to retrieve horizontal fields of τ with a spatial resolution of less than 10 m. The retrieved fields of τ were then applied to investigate horizontal cloud inhomogeneities of subtropical cirrus (index ci) and Arctic stratus (index st)."

"[…] Despite of assuming plane-parallel clouds in the simulations, the investigation of 3D radiative effects is still possible using the retrieved fields of τ, but directional features related to the scattering phase function are avoided. […]"

6. **Decorrelation length ξτ**. I wonder why did you use 1/e for the squared autocorrelation function rather than $1/e^2$.

We thank the reviewer for this advice. Now, we have used this new threshold to recalculate the decorrelation lengths, revised the relevant figures, tables, and text parts. However, the overall conclusion we made on behalf of the decorrelation lengths has not changed. Only the magnitude of the derived values for the decorrelation lengths have changed. Therefore, here in this reply, we only like to show the revised Figure 4. The remaining changes to the manuscript with regard to new decorrelation length values are marked in the additionally submitted author's response document.
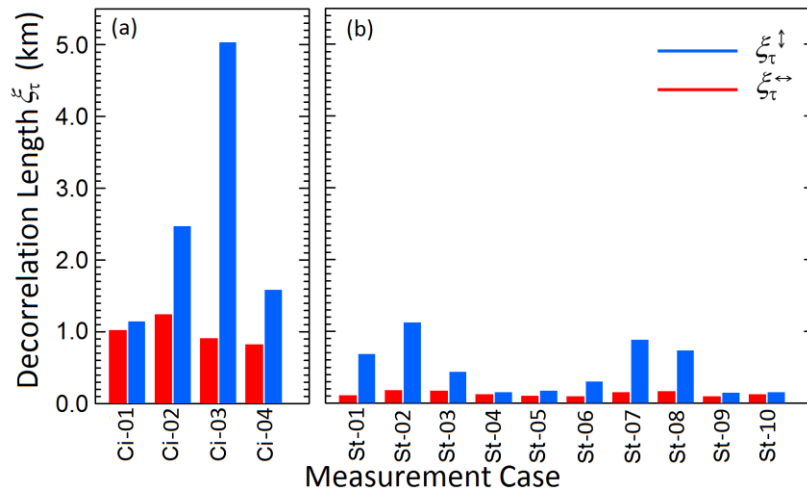

Fig. 1: Revised Fig. 4 using the new threshold for calculating the decorrelation length.

We thank the reviewer for the helpful comments which improved the manuscript significantly. The detailed replies on the reviewer's comments are given below and structured as follows. Reviewer comments have bold letters, are labeled, and listed always in the beginning of each answer followed by the author's comments including (if necessary) revised parts of the paper. The revised parts of the paper are written in quotation marks and italic letters.

Comments:

1. **Abstract – there are too many technical terms in the abstract. While reading it, it was not clear to me what the "decorrelation lengths" and "scale breaks" refer to (lines 11 to 14), and without further context, I did not know what the authors meant by "directional cloud inhomogeneities". All became clear having read the paper, although this defeats the point of the abstract – it should be a standalone block of text that is entirely contained. These terms need clarification in the abstract.**

We have revised the Abstract accordingly to make it easier to understand for the reader. Now, we have tried to avoid the technical terms.

"Clouds exhibit distinct horizontal inhomogeneities of their optical and microphysical properties, which complicate their realistic representation in weather and climate models. In order to investigate the horizontal structure of cloud inhomogeneities, two-dimensional (2D) horizontal fields of optical thickness (τ) of subtropical cirrus and Arctic stratus are investigated with a spatial resolution of less than 10 m. The 2D τ-fields are derived from (a) downward (transmitted) solar spectral radiance measurements from the ground beneath four subtropical cirrus clouds, and (b) upward (reflected) radiances measured from aircraft above ten Arctic stratus clouds. The data were collected during two field campaigns: (a) Clouds, Aerosol, Radiation, and tuRbulence in the trade wInd regime over BArbados (CARRIBA), and (b) VERtical Distribution of Ice in Arctic clouds (VERDI). One-dimensional (1D) and 2D autocorrelation functions, as well as power spectral densities are derived from the retrieved τ-fields. The typical spatial scale of cloud inhomogeneities are quantified for each cloud case. Similarly, the scales at which three-dimensional (3D) radiative effects influence the radiance field are identified. In most of the investigated cloud cases considerable cloud inhomogeneities with a prevailing directional structure are found. In these cases, the cloud inhomogeneities favour a specific horizontal direction while across this direction the cloud is of homogeneous character. The investigations reveal that it is not sufficient to quantify horizontal cloud inhomogeneities by 1D inhomogeneity parameters; 2D parameters are necessarily required."

2. **Section 1 – the authors cover a great deal of literature in this section, although in places in a somewhat haphazard manner – they may want to have another think about the structure of the section. See following comments.**

According to the reviewer's comments, we have restructured Section 1. Please find our changes below the particular comments.

3. **A) Lines 41 to 42 – to me it is unclear what the sentence "a variability of cirrus albedo of up to 25% due to spatial cirrus inhomogeneity" means. I assume it refers to a plane-parallel bias, although the sentence appears in advance of the discussion of the plane-parallel approximation (from line 46).**

That is true. The necessary information on the plane-parallel bias were missing in this sentence. We revised it as follows:

"For example, in the cases of cirrus, Carlin et al. (2002) found a plane-parallel cirrus albedo bias of up to 25 % due to spatial cirrus inhomogeneity."

B) Lines 46 to 60 – this paragraph is very muddly and confusing. It starts off introducing the plane-parallel approximation, before jumping to the independent pixel approximation, which they say is used in 1D radiative transfer calculations, but it follows after a mention of GCMs, perhaps suggesting that the IPA is used in GCMs. This paragraph should be reworded such that the distinction is clearer. The paragraph continues to cite 50% and 8% errors from two different studies, although no comment is made as to why these are so different.

We agree on that. Especially, the reference to GCMs were confusing. Furthermore, the reference to Shonk and Hogan (2008) may have been confusing at this point. With respect to other reviewer comments we agreed that this citation was rather irrelevant at this point. Therefore, we removed it and revised the relevant parts.

"Several independent studies investigated the influence of the plane-parallel assumption on cloud retrievals (e.g. Cahalan, 1994; Loeb and Davies, 1996; Marshak et al., 1998; Zinner et al., 2006; Varnai and Marshak, 2007). They found that the magnitudes of model biases are related to the degree of horizontal photon transport. In 1D radiative transfer simulations clouds are divided into separate vertical columns with horizontal homogeneous optical and microphysical properties (independent pixel approximation, IPA). However, horizontal photon transport cannot be neglected in case of inhomogeneous clouds. Additionally, multiple scattering due to 3D microphysical cloud structures smooth the horizontal radiation field. On small scales, this limits the accuracy of IPA. For example, Cahalan (1994) and Marshak et al. (1995) revealed discrepancies for individual pixel radiances exceeding 50 % due to a plan-parallel bias."

"In many remote-sensing applications clouds are assumed as plane-parallel (Francis et al., 1998; Iwabuchi and Hayasaka, 2002; Garrett et al., 2003), which may introduce biases into the modeled radiation budget (Shonk et al., 2011). For example, in the cases of cirrus, Carlin et al. (2002) found a plane-parallel cirrus albedo bias of up to 25 % due to spatial cirrus inhomogeneity. For Arctic stratus over variable sea-ice surfaces, Rozwadowska and Cahalan (2002) reported a plane-parallel albedo bias of less than 2 %, but an absolute value of the transmittance bias that can exceed 10 %."

4. Lines 64 to 68 – there is some confusion in this paragraph. It starts with a mention of Monte Carlo simulations, and then suddenly into cloud overlap schemes, which are a completely different area to horizontal cloud inhomogeneity. The authors also assert that Tripleclouds is a cloud overlap scheme – this is not true: it is a method for representing horizontal cloud inhomogeneity in GCMs. Additionally, the scheme is called "Tripleclouds", not "Triplecloud". The following description of Huang and Liu's (2014) method is also not clear. This part of the literature review may need restructuring – as the paper is dealing with metrics of horizontal inhomogeneity, it would be better to introduce methods of accounting for horizontal inhomogeneity in a more clear manner – plus the authors may want to include the Monte-Carlo ICA method of Pincus et al (2003).

The reviewer is right. Talking about cloud overlap schemes at this point is misleading. Therefore, we removed those parts, which are related to cloud overlap schemes, in the resubmitted version of the manuscript. Furthermore, we followed the suggestion of the reviewer and included the Monte Carlo ICA method of Pincus et al. (2003).

"3D Monte Carlo radiative transfer simulations account for horizontal photon transport (Barlakas et al., 2016). However, they are costly in terms of computation time and memory (Huang et al., 2014). This renders Monte Carlo radiative transfer simulations inappropriate for the application in operational or global models. Other approaches introduce Monte Carlo integration of independent column approximation (McICA), as proposed by Pincus et al. (2003). McICA is a computational efficient technique for computing domain-averaged broadband radiative flux densities in vertically and horizontally variable cloud fields (Pincus et al., 2003). Improvements compared to the plane-parallel assumption are achieved with this approach, but results are still not as accurate as those from 3D Monte Carlo models. To reduce uncertainties associated with the 1D plane-parallel assumption, Huang et al. (2014) apply spatial autocorrelation functions of cloud extinction coefficients to capture the net effects of sub-grid cloud interactions with radiation. With several orders less computation time, this approach reproduces 3D Monte Carlo radiative transfer simulations with an accuracy within 1 %. However, Huang et al. (2014) assumed perfect knowledge about the spatial correlation functions of cloud extinction coefficients, which underlines the need for measurements of comparable resolved inhomogeneity measures."

5. Line 75 – why has the ECMWF mode been singled out as an example here? Surely all models need sub-grid scale parameterisations of cloud structure.

There is no specific reason why ECMWF has been singled out as an example here. Therefore, in the resubmitted version of the manuscript we have decided to single out no special model.

"General circulation or numerical weather forecast models require sub-grid scale parameterizations of, e.g., cloud structures, liquid water content (LWC), and/or ice water content (IWC) (Huang and Liu, 2014)."

6. Line 84 – the authors say that 1D measures of inhomogeneity can lead to unrealistic results. To describe them as unrealistic does not really feel fair. A 2D metric of horizontal cloud structure is more descriptive of the cloud field, but 1D metrics can still provide information about the "bulk" structure of the cloud field over all angles.

The reviewer is right. "Unrealistic" is a rather hard wording in this context. Therefore, we have revised this paragraph in the following way:

"[…] In such a case, 1D observations with LIDAR (light detecting and ranging) or point spectrometers can lead to an underestimation or overestimation of the degree of cloud inhomogeneity of the whole cloud scene. For example, a cloud with a rather inhomogeneous character may be classified as horizontally homogeneous (underestimation of inhomogeneity), if the dominating cloud structure has the same orientation as the cloud observational path. Contrary, the cloud inhomogeneity would be overestimated if the cloud is scanned perpendicular to the major directional structure. […]"

7. Lines 90 to 94 – the entire scope and contents of the paper are summed up into a short paragraph of four lines. The contents of the paper could be described in a little more detail. Also, this paragraph (and indeed section 1) is lacking in aims and motivations of the study – indeed, all it says is what the authors will do in their paper, with no science questions. This needs expanding.

Indeed, the entire scope and contents of the paper were summed up into a quite short paragraph. We revised this part and included more information.

"In this paper, horizontal τ fields retrieved from solar spectral radiance measurements are analyzed to quantify horizontal inhomogeneities of two cloud types; subtropical cirrus and Arctic stratus. The information content of 1D and 2D approaches on cloud inhomogeneity analysis are compared to identify their scientific value and limits. In Sect. 3, a statistical evaluation of the horizontal inhomogeneity of the fields of τ is presented using common 1D inhomogeneity parameters from the literature. Those bulk properties are valid to quantify the overall cloud inhomogeneity, but cannot reproduce spatial inhomogeneities of the cloud field. In Sect. 4, the derived bulk properties from the 1D inhomogeneity parameters are compared to 1D and 2D autocorrelation functions. Finally, in Sect. 5, 1D and 2D Fourier analysis is used to investigate the effect of horizontally cloud inhomogeneities on radiative transfer."

8. **Lines 99 to 100 – this is not a particularly important point, but it would be great to get a better idea of how the scans are made – for example, are they made from a long time series of 1D scans across a path, or are they full 2D scans that overlap? The papers referred to here probably describe this fully, but it would be nice to have a little more information here.**

Indeed, the measurement technique was described a bit to briefly. Now, we have included more information on that, which should help the reader to better understand how the measurements where performed.

"[…] Two-dimensional (2D) fields of downward and upward solar spectral radiances ($I^{\downarrow}_{\lambda}$, $I^{\uparrow}_{\lambda}$) were measured from the ground (CARRIBA) and from an aircraft (VERDI). The imaging spectrometer AisaEAGLE (manufactured by Specim Ltd., Finland, Hanus et al., 2008; Schäfer et al., 2013, 2015) was used for the measurements. It is a single-line sensor with a field of view of 37° and 1024 spatial pixels detecting radiation in the wavelength range from 400 nm to 970 nm with a spectral resolution of 1.25 nm full width at half maximum (FWHM). The 2D scans of the cloud scenes are generated from sequential (4 Hz to 30 Hz frame rate) measurements of the single sensor-line, while the target (cloud) moves with the wind (ground-based) or the flying aircraft across this sensor line. Adding up all measured lines behind each other, the 2D scan evolves as an image with a spatial (number of sensor pixels) and temporal (number of recorded frames) axis. Applying the known geometry, integration time, cloud and aircraft velocities, the axes dimensions can be transferred into distances. The 2D images evolved either from the heading of the clouds above the sensor line (ground-based), or by the movement of the sensor-line itself above the clouds (airborne). […]"

9. **Lines 115 to 121 – the wording of this argument is not particularly clear. I think the authors are saying that optical depth is better to use for this analysis because it is not dependent on scattering angle, while radiance is more directional. This could be better explained.**

Now, we have revised this paragraph to make it better understandable to the reader.

"As proposed by Marshak et al. (1995), Oreopoulos et al. (2000), or Schröder (2004), horizontal cloud inhomogeneities are studied by scale analysis of cloud-top reflectances. However, radiance measurements include the information of the scattering phase function (e.g., forward/backward scattering peak, halo features) in the measured fields of radiance (Schäfer et al., 2013). To avoid artefacts in the scale analysis resulting from such features, parameters that are independent on the directional scattering of the cloud particles have to be analyzed. The cloud optical thickness τ does not include the fingerprint of the scattering phase function. Therefore, the ground-based and airborne measured fields of $I^{\downarrow}_{\lambda}$ (CARRIBA) and $I^{\uparrow}_{\lambda}$ (VERDI) were used to retrieve horizontal fields of τ with a spatial resolution of less than 10 m. The retrieved fields of τ were then applied to investigate horizontal cloud inhomogeneities of subtropical cirrus (index ci) and Arctic stratus (index st)."

10. Line 142 – the authors say that the normalised inhomogeneity parameter can exceed one in some cases, and that this could lead to misinterpretation. I am not sure what they mean by misinterpretation – mathematically, it can happen.

That is true. There is nothing wrong with values greater than unity. This wording belonged to a former version of the manuscript, where we wanted to say that there is no upper limit for ρ_τ where the clouds can be found to be inhomogeneous to 100 %. We revised this part by the following:

"However, ρ_τ has no predefined upper limit, which might lead to misinterpretations in a variability analysis. This renders ρ_τ not as a quantitative, but qualitative measure only."

11. Page 7 – through much of this page, the authors compare the different measures of 1D inhomogeneity from their study with values from other studies and say that they "compare well" and similar. It should be noted that these inhomogeneity parameters can be highly related to the domain and pixel size of the observations in the studies (see Shonk et al 2010, part one). To say that values "compare well" is probably only fair to use when comparing with studies that use very similar domain/pixel sizes. The same is also true in the conclusions in lines 398 to 399.

We thank the reviewer for this advice. Indeed, a comparison of the results is complicated for different pixel and domain sizes. However, we still like to show and refer the results from other studies. Therefore, we kept this comparison, but we included a paragraph, which points out the restriction of a comparison. The reader has to keep in mind that the results from the different studies are related to different pixel and domain sizes. Furthermore, we included the pixel and domain size of the investigated cases in Table 1 and added the pixel and domain sizes for the literature cases at the relevant parts.

"The three 1D inhomogeneity parameters ρ_τ, S_τ, and χ_τ are calculated for each retrieved field of τ_{ci} and τ_{st} from the CARRIBA and VERDI campaigns. The results are listed in the right three columns of Tab. 1. When comparing them to literature values one has to keep in mind that cloud inhomogeneities appear on different spatial scales. E.g., cloud fields may change on synoptic scales (~ 100 km) or dynamic scales (10 – 100 m) depending on the cloud type. Therefore, inhomogeneity parameters depend on the pixel and domain size of the analyzed cloud fields. The larger the domain size or the smaller the pixel size is, the broader the probably density function of the cloud parameter may become. Therefore, a comparison of different cloud cases is only valid when pixel size and cloud domain are in the same range."

We also revised this statement in the conclusion part of the manuscript:

"Considering the pixel and domain size of the analyzed measurements, the results from the calculated 1D inhomogeneity parameters ρ_τ, S_τ, are in agreement with values given in the literature for similar cloud types."

12. **Line 204 – the authors take the square of the autocorrelations to get an absolute correlation, which is fine, although I would contend that finding negative correlations is not necessarily ambiguous.**

The reviewer is right. The use of the word "ambiguous" is not suitable for the statement we wanted to give here. We revised the paragraph by the following lines to clarify what we wanted to say at this point:

"Here, only the degree of correlation matters; the positive or negative sign of the autocorrelation result is of less importance. To avoid misinterpretations with the sign, the squared autocorrelation function $P^2_\tau(L_x,L_y)$ is used here. "

13. **Line 209 – if the positive and negative signs indicate the shifting direction, I would say they do have physical meaning.**

To avoid confusion, we revised the part by the following sentence:

"The positive and negative signs of L_x and L_y in Fig. 2b and 2d illustrate the direction into which one the particular image is shifted against itself to derive the depicted autocorrelation coefficients."

14. **Figure 3 – this caption could do with a little more information. The caption is entirely written in mathematical terms – it is clear what these mean by reading the text, but defining them briefly in the caption could be helpful.**

We have extended the content of the figure caption with more information and also included the words for the single symbols to make it better readable.

"Figure 3. (a) Average of squared 1D autocorrelation functions $P^2_\tau(L_x;L_y)$ (solid lines), calculated for pixels, which are orientated into the direction of the blue (L_x) and red line (L_y) illustrated in Fig. 2b. The dashed lines mark the derived distance of the decorrelation length ξ_τ, where $P^2_\tau(L_x)$ and $P^2_\tau(L_y)$ are decreased to $1/e^2$. (b) Same as (a) for $P^2_\tau(L_x;L_y)$ shown in Fig. 2d."


15. **Figure 4 – why are the red and blue bars stacked? This gives the impression that the authors are summing together the Lx-direction and Ly-direction decorrelation length scales – by the looks of Table 2, this is not the case. I assume they have been arranged in this way because the blue bar is always taller, implying that the decorrelation length in the Ly-direction is always greater. (Which itself is an interesting question that is not addressed.)**

The reviewer is right. We revised this figure (also with respect to comments of the other reviewers) and put the bars next to each other. Please find the revised Fig. 4 below. The reason for the systematic larger blue bars in each measurement case is that these are the calculations for the decorrelation lengths along the prevailing directional structure of the

cloud inhomogeneities, while the red bars are the calculations for the decorrelation lengths across those prevailing directional structures. To make this more clear we revised a few text parts:

"The decorrelation lengths are calculated for each measurement case of CARRIBA and VERDI along ($\xi_\tau^\updownarrow$) and across ($\xi_\tau^\leftrightarrow$) the prevailing directional structure of the cloud inhomogeneities, which is identified by the 2D autocorrelation analysis. […]"

"[…] Furthermore, the results indicate that for most of the measurement cases from CARRIBA and VERDI a distinct directional structure of cloud inhomogeneities is observed. The results for $\xi_\tau^\updownarrow$ are in 9 of the 14 investigated cases more than twice as large as for $\xi_\tau^\leftrightarrow$."
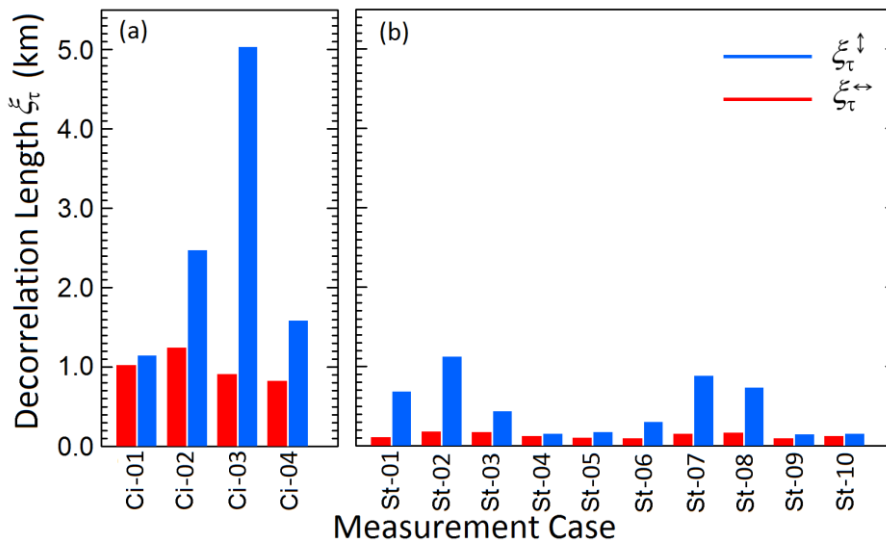
Revised Fig. 4

16. Lines 256 to 257 – the authors provide a conclusion for section 4 with the sentence "A comparison can only indicate … inhomogeneities." Many aspects of this sentence are unclear – indeed, I am not sure what the authors are concluding.

The sentence was probably too short with too less information. Now we have extended this part by the following:

"However, the absolute values of $\xi_\tau^\updownarrow$ and $\xi_\tau^\leftrightarrow$ for the Arctic stratus are smaller (more inhomogeneous) than those for the subtropical cirrus, although the 1D inhomogeneity parameters from Tab. 1 yield similar values. This reveals that the 1D inhomogeneity parameters ρ_τ, S_τ, and χ_τ just provide incomplete information for a comparison of different types of clouds as they are not able to consider the horizontal structure of cloud inhomogeneities. Differences can only be observed by an evaluation of the horizontal pattern of the cloud inhomogeneities."

17. Lines 348 to 352 – the authors introduce the reduced noise terms, but again perhaps a little too technically for someone who does not know how to do it – they may want to consider revising these few lines to make the method clearer.

We have now included the relevant equations for the octave binning. This should help the reader to understand the method easier.

"To evaluate the resulting 1D Fourier spectra with reduced noise (rn) characteristics, the $E_{rn}(k) \sim k^{\beta}$ are calculated with the use of octave binning, following the method proposed by Davis et al. (1996), Harris et al. (1997), and Schröder (2004). Logarithmically spaced bins k_n are calculated by:

$$k_n = \frac{1}{2^n} \sum_{i=2n}^{2^{n+1}-1} k_i, n = 1, 2, ..., \log_2(N-2),$$

for the number of data points N. $E(k_{rn})$ is then obtained by:

$$E(k_{\text{rn}}) = \frac{1}{2^n} \sum_{i=2n}^{2^{n+1}-1} E(k_i), n = 1, 2, ..., \log_2(N-2).$$

Within each bin 2^n data points are averaged. In addition to the reduced noise of $E(k_{rn})$ compared to $E(k_y)$ the binning provides a uniform contribution of all scales to the average values. The $E(k_{rn})$ derived from the octave binning are included as green diamonds in Fig. 6. The data of the octave binning were used to fit the spectra for different slopes in the different scale ranges."

18. Line 375 – is the CARRIBA cirrus "more homogeneous" than the VERDI stratus? Earlier, the authors say that cases C-02 and C-03 are more homogeneous than C-01 and C-04, and in Table 2, we see that they have larger decorrelation length scales. But the decorrelation scales from the VERDI stratus are smaller than those from the CARRIBA cirrus, which surely means that the cirrus are more inhomogeneous than the stratus? Or am I missing something?

We admit that this might be confusing, but the subtropical cirrus is more homogeneous than the Arctic stratus. Like the reviewer said for the subtropical cirrus cases, larger decorrelation lengths are related to more homogeneous clouds (Ci-02 and Ci-03 have a larger decorrelation length than Ci-01 and Ci-04 and are more homogeneous). The Arctic stratus cases in turn have an overall smaller decorrelation length than the subtropical cirrus cases for the spatial domain investigated here. Thus, they are more inhomogeneous than the subtropical cirrus cases. This is related to the fact that homogeneous clouds show a similar horizontal structure over a larger spatial range than inhomogeneous clouds. Therefore, from the autocorrelation analysis the inhomogeneous clouds are decorrelated at smaller spatial scales than the homogenous clouds, which relates to smaller decorrelation length.

19. **Line 408 – I think this first sentence is saying that, when determining cloud inhomogeneity, it is important to consider the full horizontal structure of clouds via a 2D metric rather than a 1D metric. The authors may want to revisit this sentence – at the moment, it seems to imply that performing 2D analysis shows that 1D analysis works.**

It is true. The sentence was written the wrong way around. We revised those lines. Now the message should become clear.

"However, the comparison of the 2D analysis of squared autocorrelation functions $P^2_\tau(Lx;Ly)$ with the 1D inhomogeneity parameters ρ_τ, $S\tau$, and χ_τ showed that it is important to consider the full horizontal structure of clouds using 2D analysis rather than 1D analysis, when determining cloud inhomogeneity."

20. **Lines 443 to 444 – the final conclusion seems to be that, despite having gone to all the trouble of calculating several different measures of 1D and 2D inhomogeneity, "the directional structure of cloud inhomogeneities generally should be taken into account". This feels like a weak concluding comment. For a start, what is meant by "generally"? Clearly some clouds will have less directional dependence of cloud inhomogeneity, but this does not mean it is not useful to measure it. How is best to determine this two-dimensional inhomogeneity? Which of the methods compared performed best? Which is easiest to calculate? Which is most useful if, say, 2D inhomogeneity parameters were to be included in a climate model? Also, how easy is it to obtain observational cloud data to extract these 2D cloud fields – are they readily available, or should we be carrying out more of these field campaigns to build up a better idea of cloud inhomogeneity? And is there any cause to investigate 3D cloud inhomogeneity metrics? These are a few questions that popped up in my mind having read the paper – it is disappointing that the authors have not included any such consideration on the implications of these results on the scientific community, and how the work could be taken forward.**

The reviewer is right. So far in the manuscript we had included to less information on the feasibility of the study and possible applications of the presented investigations. We revised the conclusion part to make the most important results more clear and we further tried to address the questions raised by the reviewer.

"[…] Furthermore, the results from the 2D analysis showed that for the observed cloud cases the subtropical cirrus was more homogeneous than the Arctic stratus. This result was not available from the investigation of the commonly used 1D inhomogeneity parameters. Therefore, using 2D methods in future studies for the characterization of cloud inhomogeneities is advisable, since their information content exceeds the information content of the commonly used 1D inhomogeneity parameters. Nowadays, 2D images of cloud fields are widespread by e.g., measurements of all-sky cameras or satellite observation with high spatial resolution. Applying the presented methods to such continuous measurements would provide detailed views into the climatology of cloud inhomogeneities. […]"

"[…] We found such differences for more than the half of the observed cloud scenes. Therefore, the directional structure of cloud inhomogeneities should be taken into account, when cloud inhomogeneities are characterized. Clearly some clouds will have less directional dependence of cloud inhomogeneity, but this does not mean it is not useful to measure it. It is expected that the information content derived from the directional analysis of cloud inhomogeneities can clearly improve sub-grid scale parametrizations in weather and climate models. For this, depending on the application, the decorrelation length (size and structure of cloud inhomogeneities) or the scale breaks (horizontal photon transport, 3D radiative effects) may provide better proxies compared to commonly used 1D inhomogeneity parameters.

However, so far only two cloud types were investigated. To build up a better idea on cloud inhomogeneity of different cloud types, more high definition observations of cloud fields are needed. Beside dedicated field campaigns, continuous observations by all-sky cameras or satellites with high spatial resolution such as LandSat (15-90 m resolution) or ASTER (Advanced Spaceborne Thermal Emission and Reflection Radiometer, 15-90 m resolution) may provide the required data.

The 1D and 2D autocorrelation functions and Fourier analysis in conjunction with the derived decorrelation length and scale breaks are a helpful tool to verify cloud resolving models in terms of typical horizontal cloud geometries."

Specific comments:

1. **Line 9 and 97 – should "VERical" read "VERtical" (or is it spelt like that in the project name)?**

Changed to *"VERTical"*

2. **Line 105 – ""…full width at…", not "…full with at…".**

Changed to *"full width at…"*

3. **Table 1 – the four cirrus cases are all labelled "C-01" – should these be "C-01", "C-02", and so on?**

We corrected the numbering. We further renamed it to Ci-01,… and St-01,…

4. **Line 192 – "both dimensions", not "both dimension".**

Changed to *"both dimensions"*

5. Figure 4 – "Decorrelation" on the y-axis has been written as "De-Correlation".

Changed to *"Decorrelation"*

6. Line 239 and 247 – the value of 3154 m is shown as 3153 m in Figure 3.

The calculated value was 3153.8 m. in the text we have used the rounded value 3154 m. In the Figure just the decimal place was cut. However, using the new threshold of $1/e^2$ for the calculation of the decorrelation lengths the, the whole value has changed and was revised.

7. Line 262 – "in a horizontal direction", not "in horizontal direction".

Changed to *"in a horizontal direction"*

8. Lines 304 to 305 – "Ea and Eb" has been written as "Ea and Ea".

Changed to *"E_a and E_b"*

9. Lines 328 and 329 – "inhomogeneity" has been written twice as "inhomogeniety".

Both changed to *"inhomogeneity"*

10. Line 337 – "too small", not "to small".

Changed to *"too small"*

11. Line 346 – "overlaid", not "overlayed".

Changed to *"overlaid"*

12. Line 360 "decreases to 2.2" should be "decreases to –2.2" (based on the numbers on Figure 6).

Changed to *"-2.2"*

13. Figure 7 – the caption seems to be a copy of the caption of Figure 6.

We have revised this mistake.

"Figure 7. Across swath derived large scale breaks ξ_{τ_L} for the retrieved fields of τ from the (a) CARRIBA (Ci- 01 to Ci-04, red) and (b) VERDI (St-01 to St-10, blue) campaigns. The values were derived by using the method presented in Fig. 6."

14. Line 408, 411 and 435 – the authors switch here between P and P^2 – is there any reason for this?

We used P and not P^2 at the relevant parts because at this point we talked about general properties of autocorrelation functions. At the point where it comes to the decorrelation length we changed it to P^2. However, since this may be confusing we revised the relevant parts and directly talk about P^2.

15. Line 473 – "Green-function", not "green-function" (I think they are named after someone called Green).

Changed to *"Green-function"*

16. Line 480 – "absorption", not "absorbtion".

Changed to *"absorption"*

17. Lines 524 and 526 – check the spelling of "Schroeder" vs "Schröeder".

Both changed to *"Schröder"*

18. Line 538 – "Earth's", not "Earths".

Changed to *"Earth's"*

19. Finally, the authors have started several sentences throughout the paper with numbers and variables – this is something that may get picked up later in the review process, but they may want to revise these sentences so that they start with words.

We have checked the whole manuscript for such cases and reworded the sentences, which started with a number or variable.

Directional, Horizontal Inhomogeneities of Cloud Optical Thickness Fields Retrieved from Ground-Based and Airborne Spectral Imaging

Michael Schäfer[1], Eike Bierwirth[1,2], André Ehrlich[1], Evelyn Jäkel[1],
Frank Werner[3], and Manfred Wendisch[1]

[1]Leipzig Institute for Meteorology, University of Leipzig, Leipzig, Germany
[2]now at: PIER-ELECTRONIC GmbH, Nassaustr. 33–35, 65719 Hofheim-Wallau, Germany
[3]Joint Center for Earth Systems Technology, University of Maryland, 5523 Research Park Drive 320, Baltimore, MD 21228

Correspondence to: Michael Schäfer (michael.schaefer@uni-leipzig.de)

Abstract. Clouds exhibit distinct horizontal inhomogeneities of their optical and microphysical properties, which complicate their realistic representation in weather and climate models. In order to investigate the horizontal structure of cloud inhomogeneities, two-dimensional (2D) horizontal fields of optical thickness (τ) of subtropical cirrus and Arctic stratus are investigated with a spatial

5   resolution of less than 10 m. The 2D τ-fields are derived from (a) downward (transmitted) solar spectral radiance measurements from the ground beneath four subtropical cirrus clouds, and (b) upward (reflected) radiances measured from aircraft above ten Arctic stratus clouds. The data were collected during two field campaigns: (a) Clouds, Aerosol, Radiation, and tuRbulence in the trade wInd regime over BArbados (CARRIBA), and (b) VERtical Distribution of Ice in Arctic clouds (VERDI). One-

10   dimensional (1D) and 2D autocorrelation functions, as well as power spectral densities are derived from the retrieved τ-fields. The typical spatial scale of cloud inhomogeneities are quantified for each cloud case. Similarly, the scales at which three-dimensional (3D) radiative effects influence the radiance field are identified. In most of the investigated cloud cases considerable cloud inhomogeneities with a prevailing directional structure are found. In these cases, the cloud inhomogeneities favour

15   a specific horizontal direction while across this direction the cloud is of homogeneous character. The investigations reveal that it is not sufficient to quantify horizontal cloud inhomogeneities by 1D inhomogeneity parameters; 2D parameters are necessarily required.

1 Introduction

The globally and annually averaged cloud cover is in the range of about $70\,\%$ (Rossow and Schiffer,

20   1999). Because of this high percentage, and their important effects on the Earth's radiation budget, clouds need to be considered as an important regulator of the Earth's climate (Albrecht, 1989; Loeb et al., 2009). Clouds scatter and absorb solar radiation in the wavelength range from $0.2\,\mu\text{m}$ to $5\,\mu\text{m}$; they emit and absorb terrestrial radiation from $5\,\mu\text{m}$ to $50\,\mu\text{m}$. Although clouds have been studied for several decades, they are still poorly represented in weather and climate models (Shonk et al.,

25   2011). The latest report of the Intergovernmental Panel on Climate Change (IPCC, 2013) classifies cloud effects as one of the largest uncertainties in climate simulations, significantly contributing to problems in the determination of the Earth's energy budget (Stocker et al., 2013). These issues partly arise from an unrealistic representation of complex horizontal cloud structures and from cloud-radiation feedback processes that control the cloud evolution (Stephens, 2005; Shonk et al., 2011).

30   Therefore, the representation of cloud inhomogeneities needs to be become more realistic (Shonk et al., 2011). This is particularly important, because changes of cloud properties may have serious consequences on the interaction of clouds with radiation (Slingo, 1990).

Several independent studies investigated the influence of the plane-parallel assumption on cloud retrievals (e.g. Cahalan, 1994; Loeb and Davies, 1996; Marshak et al., 1998; Zinner et al., 2006; Var-

35   nai and Marshak, 2007). They found that the magnitudes of model biases are related to the degree of horizontal photon transport. In 1D radiative transfer simulations clouds are divided into separate vertical columns with horizontal homogeneous optical and microphysical properties (independent pixel approximation, IPA). However, horizontal photon transport cannot be neglected in case of inhomogeneous clouds. Additionally, multiple scattering due to 3D microphysical cloud structures smooth

40   the horizontal radiation field. On small scales, this limits the accuracy of IPA. For example, Cahalan (1994) and Marshak et al. (1995) revealed discrepancies for individual pixel radiances exceeding $50\,\%$ due to a plan-parallel bias.

High ice clouds (cirrus) and Arctic stratus exhibit horizontal inhomogeneities at different horizontal scales. Both cloud types can either warm or cool the Earth's climate system, depending on their

45   optical and microphysical properties and the meteorological conditions. For example, Choi and Ho (2006) reported for tropical regions a positive (warming) net radiative effect of cirrus for a cirrus optical thickness (τ_{ci}) of less than 10, but a cooling effect for $\tau_{\text{ci}} > 10$. For Arctic stratus, Wendisch et al. (2013) showed that for low surface albedo (α_{s}) and low solar zenith angle (θ_0), the cloud cools the sub-cloud layer. With increasing α_{s} and increasing θ_0, the cooling effect of the low–level cloud

50   turns into a warming. Both, clouds and surface reflection properties can vary significantly and in different horizontal scales.

In many remote-sensing applications clouds are assumed as plane-parallel (Francis et al., 1998; Iwabuchi and Hayasaka, 2002; Garrett et al., 2003), which may introduce biases into the modeled radiation budget (Shonk et al., 2011). For example, in the cases of cirrus, Carlin et al. (2002) found

2

a plane-parallel cirrus albedo bias of up to 25% due to spatial cirrus inhomogeneity. For Arctic stratus over variable sea-ice surfaces, Rozwadowska and Cahalan (2002) reported a plane-parallel albedo bias of less than 2%, but an absolute value of the transmittance bias that can exceed 10%.

3D Monte Carlo radiative transfer simulations account for horizontal photon transport (Barlakas et al., 2016). However, they are costly in terms of computation time and memory (Huang and Liu, 2014). This renders Monte Carlo radiative transfer simulations inappropriate for the application in operational or global models. Other approaches introduce Monte Carlo integration of independent column approximation (McICA), as proposed by Pincus et al. (2003). McICA is a computational efficient technique for computing domain-averaged broadband radiative flux densities in vertically and horizontally variable cloud fields (Pincus et al., 2003). Improvements compared to the plane-parallel assumption are achieved with this approach, but results are still not as accurate as those from 3D Monte Carlo models. To reduce uncertainties associated with the 1D plane-parallel assumption, Huang and Liu (2014) apply spatial autocorrelation functions of cloud extinction coefficients to capture the net effects of sub-grid cloud interactions with radiation. With several orders less computation time, this approach reproduces 3D Monte Carlo radiative transfer simulations with an accuracy within 1%. However, Huang and Liu (2014) assumed perfect knowledge about the spatial correlation functions of cloud extinction coefficients, which underlines the need for measurements of comparable resolved inhomogeneity measures.

General circulation or numerical weather forecast models require sub-grid scale parameterizations of, e.g., cloud structures, liquid water content (LWC), and/or ice water content (IWC) (Huang and Liu, 2014). In reality, cloud structures reveal spatial features down to distances below the meter scale (Pinsky and Khain, 2003). Therefore, measurements with appropriate spatial and temporal resolution have to be conducted in order to derive the needed parameterizations. The required measurements include cloud altitude (temperature), its geometry (vertical and horizontal extent), and cloud microphysical properties (e.g., LWC, IWC, droplet size, ice crystal size and shape distributions).

Cloud inhomogeneities often exhibit a typical directional structure (e.g., induced by the prevailing wind). In such a case, 1D observations with LIDAR (light detecting and ranging) or point spectrometers can lead to an underestimation or overestimation of the degree of cloud inhomogeneity of the whole cloud scene. For example, a cloud with a rather inhomogeneous character may be classified as horizontally homogeneous (underestimation of inhomogeneity), if the dominating cloud structure has the same orientation as the cloud observational path. Contrary, the cloud inhomogeneity would be overestimated if the cloud is scanned perpendicular to the major directional structure. Therefore, 2D observations are a useful tool to avoid such misinterpretations of cloud inhomogeneity.

In this paper, horizontal τ fields retrieved from solar spectral radiance measurements are analyzed to quantify horizontal inhomogeneities of two cloud types; subtropical cirrus and Arctic stratus. The information content of 1D and 2D approaches on cloud inhomogeneity analysis are compared to identify their scientific value and limits. In Sect. 3, a statistical evaluation of the horizontal inho-

mogeneity of the fields of τ is presented using common 1D inhomogeneity parameters from the literature. Those bulk properties are valid to quantify the overall cloud inhomogeneity, but cannot reproduce spatial inhomogeneities of the cloud field. In Sect. 4, the derived bulk properties from the 1D inhomogeneity parameters are compared to 1D and 2D autocorrelation functions. Finally, in Sect. 5, 1D and 2D Fourier analysis is used to investigate the effect of horizontally cloud inhomogeneities on radiative transfer.

2 Data Set: 2D-Fields of Cloud Optical Thickness

Data from two international field campaigns have been analyzed: the Clouds, Aerosol, Radiation, and tuRbulence in the trade wInd regime over BArbados (CARRIBA, Siebert et al., 2013; Schäfer et al., 2013) campaign performed on Barbados in April 2011, and the VERtical Distribution of Ice in Arctic clouds (VERDI, Schäfer et al., 2015) observations carried out in Inuvik, Canada in May 2012. Two-dimensional (2D) fields of downward and upward solar spectral radiances ($I_\lambda^\downarrow$, $I_\lambda^\uparrow$) were measured from the ground (CARRIBA) and from an aircraft (VERDI). The imaging spectrometer AisaEAGLE (manufactured by Specim Ltd., Finland, Hanus et al., 2008; Schäfer et al., 2013, 2015) was used for the measurements. It is a single-line sensor with a field of view (FOV) of 37° and 1024 spatial pixels detecting radiation in the wavelength range from 400 nm to 970 nm with a spectral resolution of 1.25 nm full width at half maximum (FWHM). The 2D scans of the cloud scenes are generated from sequential (4 Hz to 30 Hz frame rate) measurements of the single sensor-line, while the target (cloud) moves with the wind (ground-based) or the flying aircraft across this sensor line. Adding up all measured lines behind each other, the 2D scan evolves as an image with a spatial (number of sensor pixels) and temporal (number of recorded frames) axis. Applying the known geometry, integration time, cloud and aircraft velocities, the axes dimensions can be transferred into distances. The 2D images evolved either from the heading of the clouds above the sensor line (ground-based), or by the movement of the sensor-line itself above the clouds (airborne). The imaging spectrometer was characterized and calibrated in the laboratory to transform the AisaEAGLE's raw data (12-bit digital numbers) into radiance. The procedure of data evaluation (calibrations, corrections) follows the methods described by Bierwirth et al. (2013) and Schäfer et al. (2013, 2015).

As proposed by Marshak et al. (1995), Oreopoulos et al. (2000), or Schröder (2004), horizontal cloud inhomogeneities are studied by scale analysis of cloud-top reflectances. However, radiance measurements include the information of the scattering phase function (e.g., forward/backward scattering peak, halo features) in the measured fields of radiance (Schäfer et al., 2013). To avoid artefacts in the scale analysis resulting from such features, parameters that are independent on the directional scattering of the cloud particles have to be analyzed. The cloud optical thickness τ does not include the fingerprint of the scattering phase function. Therefore, the ground-based and airborne measured fields of $I_\lambda^\downarrow$ (CARRIBA) and $I_\lambda^\uparrow$ (VERDI) were used to retrieve horizontal fields of τ with a spatial

4

resolution of less than 10 m. The retrieved fields of τ were then applied to investigate horizontal cloud inhomogeneities of subtropical cirrus (index ci) and Arctic stratus (index st).

130   Simulations are performed with the radiative transfer solver DISORT 2 (Discrete Ordinate Radiative Transfer). Input parameters such as cloud optical properties, aerosol content and spectral surface albedo are provided by the library for radiative transfer calculations (libRadtran, Mayer and Kylling, 2005). The required profiles of thermodynamic parameters are derived from measurements from radiosondes and/or dropsondes. Despite of assuming plane-parallel clouds in the simulations, the investigation of 3D radiative effects is still possible using the retrieved fields of τ, but directional

135 features related to the scattering phase function are avoided. $I_\lambda^\downarrow$ and $I_\lambda^\uparrow$ were simulated as a function of values of τ_{ci} and τ_{st}, respectively. The simulations were performed for all scattering angles within the FOV of AisaEAGLE. Thus, simulated grids of possible $I_\lambda^\downarrow$ and $I_\lambda^\uparrow$ and corresponding τ_{ci} and τ_{st} are available for each time step of the measurements and each spatial pixel. The retrieved τ_{ci} and τ_{st} are derived by interpolating the simulated $I_\lambda^\downarrow$ and $I_\lambda^\uparrow$ to the measured value for each spatial pixel

140 using a linear interpolation. More detailed descriptions and sensitivity tests of the applied retrieval procedures are reported by Schäfer et al. (2013) for subtropical cirrus and by Bierwirth et al. (2013) as well as Schäfer et al. (2015) for Arctic stratus. Fields of cloud optical thickness are derived for four subtropical cirrus cases (τ_{ci}) and ten Arctic stratus cases (τ_{st}). Subsequently, those fields of τ_{ci} and τ_{st} are used to investigate and quantify horizontal cloud inhomogeneities.

145   Table 1 summarizes the statistical parameters of the four retrieved fields of τ_{ci} (Ci-01 to Ci-04) and the ten retrieved fields of τ_{st} (St-01 to St-10). Figure 1 illustrates example cutouts for cases St-04 and St-07, both characterized by a measurement duration of 60 s. Table 1 further provides information on the measurement time, cloud altitude (h_{cld}), field size (swath, length), and average as well as standard deviation of τ_{ci} ($\bar{\tau}_{ci} \pm \sigma_{\tau,ci}$) and τ_{st} ($\bar{\tau}_{st} \pm \sigma_{\tau,st}$). The sampled subtropical cirrus

150 fields of about 13-44 km length and 7-8 km width are determined by the time of observation and the swath covered by AisaEAGLE. For the Arctic stratus cases the average swath of the covered cloud fields has a size close to 1.3 km. The length varies from 4 km to up to 26 km. Thus, for CARRIBA and VERDI sufficiently large areas of the clouds are covered to provide a statistically firm analysis of τ_{ci} and τ_{st} and to investigate their horizontal inhomogeneities.

155 **3 1D Inhomogeneity Parameters**

The standard deviation σ_τ of the cloud optical thickness does not allow a comparison between cases with different average cloud optical thickness $\bar{\tau}$. A cloud with higher $\bar{\tau}$ can exhibit a higher standard deviation. Therefore, similarly to the studies by Barker et al. (1996), who used ratios between mean τ and the variance of τ, Davis et al. (1999a) and Szczap et al. (2000) utilized the normalized inho-

160 mogeneity measure ρ_τ to quantify the horizontal inhomogeneity of τ. It is defined by the ratio of σ_τ

5

Table 1. Label, measurement period (day and time of day in UTC), cloud top altitude, pixel size (width, length), domain size (swath, length), and average and standard deviation ($\bar{\tau} \pm \sigma_\tau$) of the retrieved fields of τ_{ci} and τ_{st} from ground-based measured CARRIBA (Ci-01 to Ci-04) and airborne measured VERDI (St-01 to St-10) cases. The flight altitude for each VERDI case is at 2920 m. The right three columns include calculated 1D inhomogeneity parameters (ρ_τ, S_τ, χ_τ) of the retrieved fields of τ. They are discussed in Sect. 3.

| Case	Day	Time (UTC)	h_{cld} (km)	Pixel Size (m)	Domain (km)	$\bar{\tau} \pm \sigma_\tau$	ρ_τ	S_τ	χ_τ
Ci-01	9 April 2011	13:26:26 – 13:37:13	11-15	≈ 7.1 x 4.8	7.3 x 15.6	0.41 ± 0.17	0.40	0.19	0.92
Ci-02	16 April 2011	13:44:29 – 14:17:42	12-15	≈ 7.8 x 5.1	8.0 x 40.5	0.28 ± 0.09	0.35	0.15	0.94
Ci-03	18 April 2011	13:43:56 – 14:17:13	13-15	≈ 8.4 x 5.5	8.6 x 44.1	0.20 ± 0.03	0.17	0.08	0.99
Ci-04	23 April 2011	16:45:10 – 17:03:12	11-14	≈ 7.1 x 3.1	7.3 x 13.3	0.05 ± 0.04	0.91	0.48	0.63
St-01	14 May 2012	20:31:47 – 20:36:31	≤ 0.90	≈ 2.7 x 2.5	1.34 x 21.28	9.93 ± 1.89	0.19	0.08	0.98
St-02	14 May 2012	20:38:04 – 20:42:09	≤ 0.85	≈ 2.8 x 2.8	1.37 x 20.83	7.82 ± 2.01	0.26	0.11	0.97
St-03	14 May 2012	20:53:26 – 20:58:30	≤ 0.85	≈ 2.8 x 3.0	1.37 x 26.85	3.82 ± 1.33	0.34	0.20	0.92
St-04	15 May 2012	18:41:53 – 18:43:58	≤ 1.00	≈ 2.6 x 2.8	1.27 x 10.50	14.34 ± 2.54	0.18	0.08	0.98
St-05	15 May 2012	21:05:10 – 21:09:24	≤ 0.93	≈ 2.7 x 2.7	1.32 x 20.22	6.35 ± 0.97	0.15	0.07	0.99
St-06	16 May 2012	19:10:56 – 19:15:56	≤ 1.00	≈ 2.6 x 2.6	1.27 x 23.10	6.52 ± 1.48	0.23	0.11	0.97
St-07	17 May 2012	16:53:23 – 16:56:06	≤ 0.25	≈ 3.6 x 2.6	1.75 x 12.74	3.04 ± 0.66	0.22	0.11	0.97
St-08	17 May 2012	17:00:59 – 17:06:15	≤ 1.00	≈ 2.6 x 2.7	1.27 x 25.65	5.48 ± 1.84	0.34	0.15	0.95
St-09	17 May 2012	17:09:28 – 17:10:38	≤ 2.25	≈ 1.0 x 2.6	0.48 x 5.46	7.07 ± 1.41	0.20	0.09	0.98
St-10	17 May 2012	18:49:26 – 18:50:16	≤ 0.23	≈ 3.6 x 2.7	1.76 x 4.10	4.15 ± 0.67	0.16	0.08	0.99

and the average value $\bar{\tau}$ of the corresponding sample:

$$\rho_\tau = \frac{\sigma_\tau}{\bar{\tau}}. \tag{1}$$

A homogeneous cloud is characterized by $\rho_\tau = 0$. Increasing values of ρ_τ indicate rising cloud inhomogeneity. However, ρ_τ has no predefined upper limit, which might lead to misinterpretations in a variability analysis. This renders ρ_τ not as a quantitative, but qualitative measure only. Therefore, Davis et al. (1999a) and Szczap et al. (2000) convert the relative variability ρ_τ into the inhomogeneity parameter S_τ as follows:

$$S_\tau = \frac{\sqrt{\ln(\rho_\tau^2 + 1)}}{\ln 10}. \tag{2}$$

In case of a log-normal frequency distribution of τ, S_τ is proportional to to ρ_τ. This is because the reflected/transmitted radiance is approximately linear to $\log \tau$ for moderate τ (for $\log \tau = 0.5$-1.5 with $\tau \approx 3$-30). Without net horizontal photon transport, moments of reflected/transmitted radiance are closely linked with moments of $\log \tau$ rather than moments of τ (Iwabuchi and Hayasaka, 2002). Therefore, S_τ quantifies the degree of cloud inhomogeneity.

6
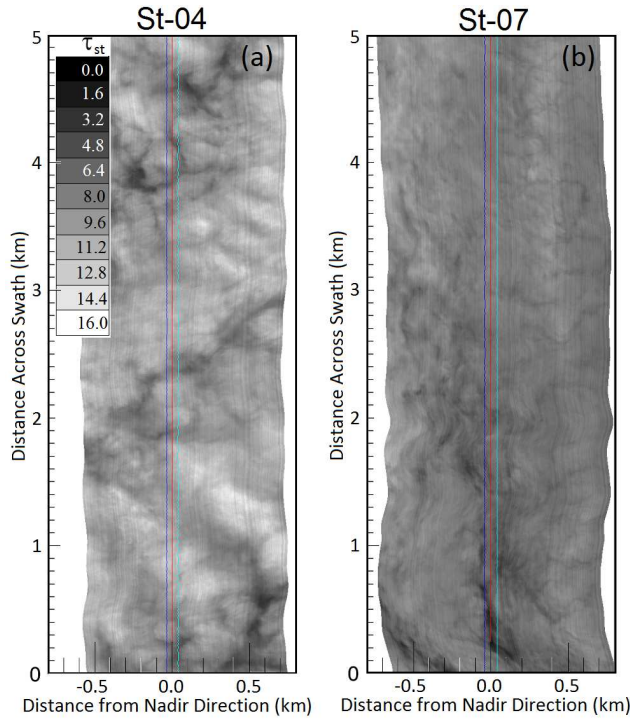
Figure 1. (a) Georeferenced field of τ_{st}. Cutout from measurement case St-04 with $60\,\mathrm{s}$ measurement duration. The dark–blue, red, and light–blue lines illustrate the nadir viewing direction in a range of $\pm 1°$. **(b)** Same as (a) for case St-07.

Oreopoulos and Cahalan (2005) investigated the inhomogeneity parameter χ_τ, first introduced by Cahalan (1994). χ_τ is defined as the ratio of the logarithmic and linear average of a distribution of $\bar{\tau}$:

$$\chi_\tau = \frac{\exp(\overline{\ln \tau})}{\bar{\tau}}, \tag{3}$$

The 1D inhomogeneity parameter χ_τ ranges between 0 and 1, with values close to unity indicating horizontal homogeneity, and values approaching zero characterizing high horizontal inhomogeneity. Oreopoulos and Cahalan (2005) state that the reflected solar flux is approximately a linear function of the logarithm of τ for a wide range of τ (≈ 3 to ≈ 30, depending on θ_0). Thus, the logarithmically averaged τ provides a way to account for cloud inhomogeneity effects in plane-parallel radiative transfer calculations using χ_τ as a scaling factor with which τ needs to be multiplied to approximate the IPA albedo.

The three 1D inhomogeneity parameters ρ_τ, S_τ, and χ_τ are calculated for each retrieved field of τ_{ci} and τ_{st} from the CARRIBA and VERDI campaigns. The results are listed in the right three columns of Tab. 1. When comparing them to literature values one has to keep in mind that cloud inhomogeneities appear on different spatial scales. E.g., cloud fields may change on synoptic scales

7

$(\approx 100\,\text{km})$ or dynamic scales $(10\text{–}100\,\text{m})$ depending on the cloud type. Therefore, inhomogeneity parameters depend on the pixel and domain size of the analyzed cloud fields. The larger the domain size or the smaller the pixel size is, the broader the probably density function of the cloud parameter may become. Therefore, a comparison of different cloud cases is only valid when pixel size and cloud domain are in the same range.

The subtropical cirrus cases observed during CARRIBA show ρ_τ in the range of 0.17–0.91, while S_τ is in the range of 0.08–0.48. The largest values of ρ_τ and S_τ are found for Ci-04, the lowest for Ci-03. The values for ρ_τ and S_τ show that the subtropical cirrus of Ci-02 and Ci-03 was quite homogeneous, whereas that of Ci-01 and Ci-04 was rather inhomogeneous. For the ten Arctic stratus cases, ρ_τ and S_τ are in the range of 0.15–0.34 and 0.07–0.20, respectively. For stratocumulus (6.9 km domain with 15 m horizontal resolution) Zuidema and Evans (1998) quantified the inhomogeneity of τ with $S_\tau = 0.1\text{–}0.3$. Iwabuchi (2000) and Iwabuchi and Hayasaka (2002) investigated the inhomogeneity of τ for overcast boundary layer clouds from a visible-wavelength moderate-resolution (about 1 km) sensor and found values of $S_\tau = 0.03\text{–}0.3$, which leads to $\rho_\tau = 0.07\text{–}0.78$. Thus, considering the different pixel and domain sizes, the derived values from CARRIBA and VERDI compare well with those reported by Zuidema and Evans (1998), Iwabuchi (2000), and Iwabuchi and Hayasaka (2002). Among all ten cases, ρ_τ and S_τ indicate case St-03 and St-08 to be more inhomogeneous.

For CARRIBA, the values of χ_τ range from 0.63 to 0.99, indicating a rather inhomogeneous cirrus for Ci-04 and quite homogeneous cirrus during the other days. In contrast to the results for ρ_τ, S_τ, and χ_τ indicate that the subtropical cirrus of Ci-01 is less inhomogeneous. The calculated values of χ_τ for the retrieved fields of τ_{st} from the VERDI campaign yield values larger than 0.9 in each case, with lowest values for case St-03 and St-08, which were already indicated by ρ_τ and S_τ to be more inhomogeneous. Using the Moderate Resolution Imaging Spectroradiometer (MODIS), depending on cloud type, cloud phase, surface type, season, and time of day, Oreopoulos and Cahalan (2005) estimate the range of χ_τ from ≈ 0.65 to 0.8 at spatial scales of $1° \times 1°$.

The 1D inhomogeneity parameters ρ_τ, S_τ, and χ_τ are easy to calculate and suitable for being implemented in simulations that assume horizontally homogeneous clouds to achieve more realistic results. They do not provide a measure of the directional variability of the inhomogeneities. However, different clouds exhibit preferred horizontal inhomogeneity patterns and typical features. For example, the clouds observed during CARRIBA and VERDI are different in terms of cloud altitude, structure, phase, particle size and shape, although ρ_τ, S_τ, and χ_τ yield comparable values (compare Fig. 1 and Tab. 1). Therefore, not only the horizontal inhomogeneity, but also the spatial coherence of cloud inhomogeneity parameters and their directional dependence need to be investigated (Hill et al., 2012).

4 Spatial 1D and 2D Autocorrelation Functions and Decorrelation Length

225 The 2D autocorrelation function $P_\tau(L_x, L_y)$ is calculated in two horizontal dimensions at fixed distances (pixel-lags) L_x and L_y, which are derived as integer multiples of the equidistant sample intervals x_j and y_k of the 2D fields of τ (Marshak et al., 1998). The maximum pixel-lags L_x and L_y are given by the number of pixels n and m of the 2D fields. Here, with n and m equidistant measurement intervals x_j and y_k, $P_\tau(L_x, L_y)$ for 2D fields of τ is calculated by:

230
$$P_\tau(L_x, L_y) = \frac{\sum\limits_{j,k+1}^{n,m} [\tau(x_j + L_x, y_k + L_y) - \bar{\tau}] \cdot [\tau(x_j, y_k) - \bar{\tau}]}{\sum\limits_{j,k+1}^{n,m} [\tau(x_j, y_k) - \bar{\tau}]^2}. \tag{4}$$

Here, $\tau(x_j, y_k)$ is the cloud optical thickness observed at the reference position, and $\tau(x_j + L_x, y_k + L_y)$ is the cloud optical thickness at pixel-lag L_x and L_y. The autocorrelation function $P_\tau(L_x, L_y)$ yields values between -1 and 1, 1 representing a perfect positive correlation (e.g., for a spatial shift equal to zero); a value of -1 is a perfect negative correlation and 0 indicates no correlation. Thus, spa-

235 tial autocorrelation functions quantify the degree of similarity between spatially distributed neighbouring samples. Usually, τ values in close horizontal distance reveal similar values, while cloud pixels at larger distances may show significantly different values of τ, depending on the cloud heterogeneity. ==Here, only the degree of correlation matters; the positive or negative sign of the autocorrelation result is of less importance. To avoid misinterpretations with the sign, the squared==

240 ==autocorrelation function $P_\tau^2(L_x, L_y)$ is used here.==

Figures 2b and 2d show examples of $P_\tau^2(L_x, L_y)$ in a 2D plot for $L_x = $ -250 to $L_x = 250$ and $L_y = $ -250 to $L_y = 250$, calculated for a selected area (500 by 500 Pixels, Figs.2a and 2b) of the cirrus fields from case Ci-01 and Ci-03 with $L_x = 250$ and $L_y = 250$. The positive and negative signs of L_x and L_y in Fig. 2b and 2d illustrate the direction into which the particular image is shifted against itself to

245 derive the depicted autocorrelation coefficients. Both cases show a different pattern of $P_\tau^2(L_x, L_y)$ with increasing absolute value of L_x and L_y. While Ci-01 shows a circular spot indicating a symmetry independent on direction, Ci-03 displays high correlation factors for all considered L_y within a range of L_x=-50 to L_x=50. This pattern indicates a homogeneous cloud structure along the y axis while the τ field along the x-axis is heterogeneous. The magnitude of decrease of $P_\tau^2(L_x, L_y)$

250 with increasing L_x and L_y depends on the horizontal structure of the cloud inhomogeneities. The $P_\tau^2(L_x, L_y)$ calculated from Ci-01 (Fig. 2b) show a decrease, independent of the direction. In contrast, the $P_\tau^2(L_x, L_y)$ calculated from Ci-03 (Fig. 2d) show a directional dependence.
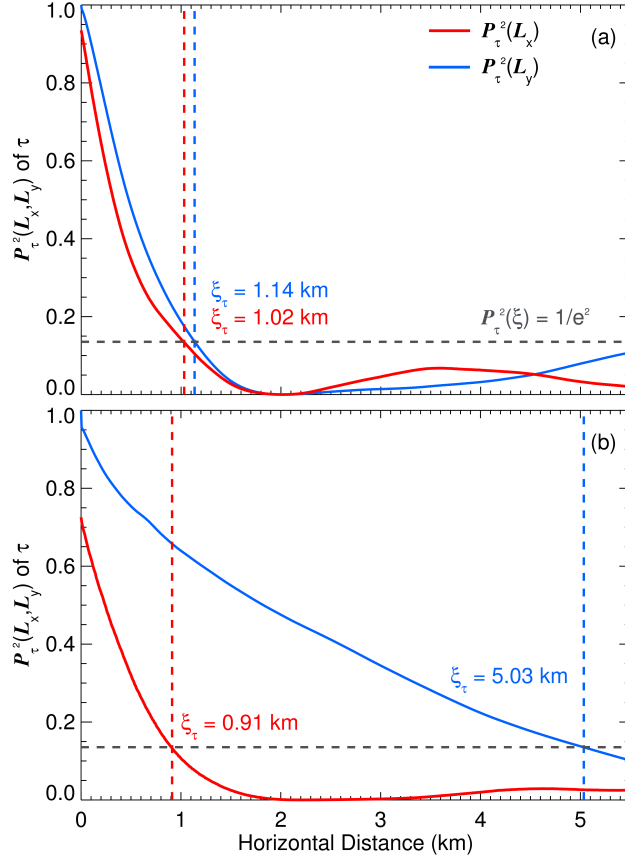
The squared spatial autocorrelation functions $P_\tau^2(L_x, L_y)$ are used to calculate the decorrelation length $\xi_\tau = \sqrt{L_x^2 + L_y^2}$ implicitly defined by:

255
$$P_\tau^2(\xi_\tau) = 1/e^2. \tag{5}$$
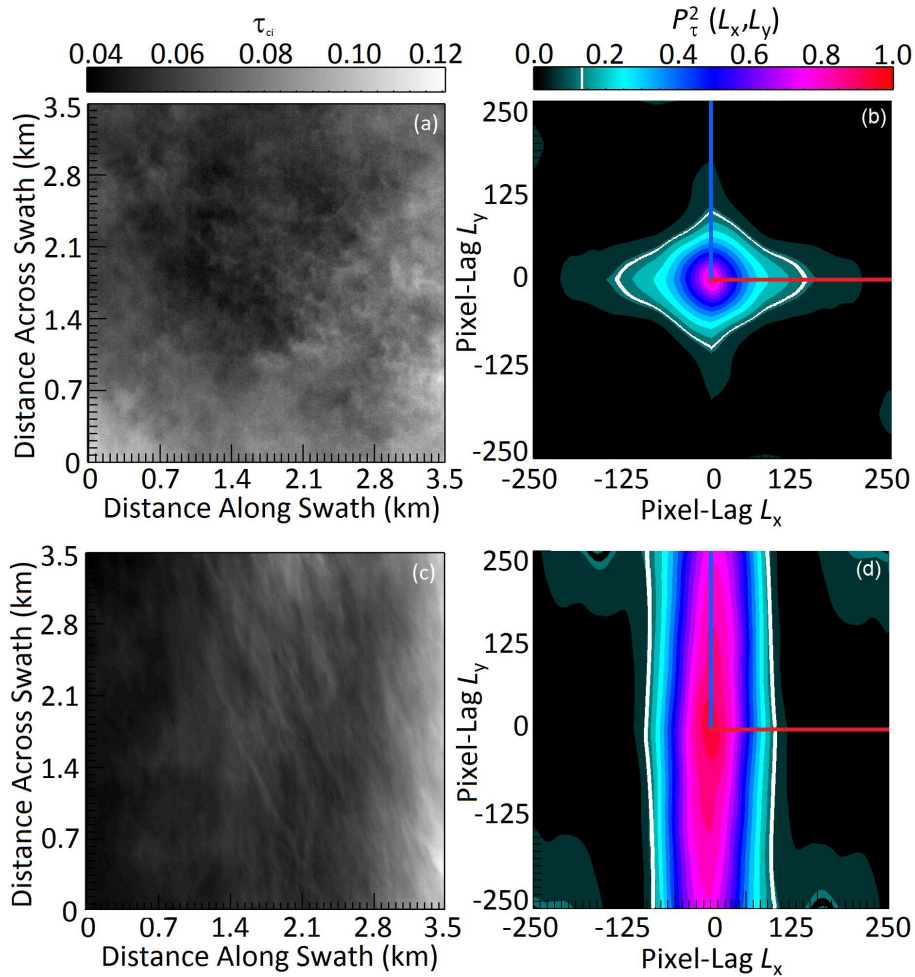
Figure 2. (a) Selected cloud scene (3.5 km by 3.5 km) of field of τ_{ci} from case Ci-01. **(b)** Color-coded 2D field of $P_\tau^2(L_x, L_y)$, calculated for field of τ_{ci} from (a). The blue and red line illustrate the pixel-lags selected for the illustration in Fig. 3a. The white line illustrates ξ_τ at $P_\tau^2(L_x, L_y) = 1/e^2$. **(c)** Same as (a) for case Ci-03. **(d)** Same as (b) for selected τ_{ci} field shown in (c).

Here, ξ_τ quantifies the length scale (in units of meter) where individual cloud parcels are decorrelated; it provides a measure of the horizontal extent of cloud inhomogeneities. Strong inhomogeneities correspond to small ξ_τ. In Figs. 2b and 2d, ξ_τ is indicated by a white line. For Ci-01 ξ_τ forms a circular shape indicating a similar magnitude of cloud inhomogeneities in all directions of the cloud field. Conversely, for Ci-03 ξ_τ along pixel-lag L_x is significantly smaller than ξ_τ along pixel-lag L_y. This directional dependence is related to the structure of the cloud with regular filaments in the swath direction of the image in Fig. 2c. For case Ci-01 the symmetry in $P_\tau^2(L_x, L_y)$ means that the cloud inhomogeneity can be characterized by a single value ξ_τ, independent of direction. For regularly structured clouds such as Ci-03, however, the 2D decorrelation can be split

260

10

Figure 3. **(a)** Average of squared 1D autocorrelation functions $P_\tau^2(L_x, L_y)$ (solid lines), calculated for pixels, which are orientated into the direction of the blue (L_x) and red line (L_y) illustrated in Fig. 2b. The dashed lines mark the derived distance of the decorrelation length ξ_τ, where $P_\tau^2(L_x)$ and $P_\tau^2(L_y)$ are decreased to $1/e^2$. **(b)** Same as (a) for $P_\tau^2(L_x, L_y)$ shown in Fig. 2d.

265   into a component of the largest variability and another one along the smallest variability of τ. In the cloud fields presented here, both major axes align with the x and y direction. 1D autocorrelation functions along the axis of strongest ($\leftrightarrow$, red line in Figs. 2b and 2d) and weakest ($\updownarrow$, blue line in Figs. 2b and 2d) variability are provided in Figs. 3a and 3b. To derive quantitative values for $\xi_\tau^{\leftrightarrow}$ and $\xi_\tau^{\updownarrow}$ in SI-units of meter, the pixel-lag is transformed into horizontal distances by multiplying the 270   number of pixels by their pixel size.

     For case Ci-01 (Figs. 2a, 2b, and 3a), the derived $P_\tau^2(L_x, L_y)$ along and across the prevailing directional structure are similar and $\bar{\xi}_\tau^{\updownarrow} = 1.14\,\text{km}$ compares well with $\bar{\xi}_\tau^{\leftrightarrow} = 1.02\,\text{km}$ within the range of standard deviation given in Tab. 2. For case Ci-03 (Figs. 2c, 2d, and 3b), the $P_\tau^2(L_x, L_y)$ along and across the prevailing directional structure differ significantly from each other and $\bar{\xi}_\tau^{\updownarrow} = 5.03\,\text{km}$ 275   is about six times larger than $\bar{\xi}_\tau^{\leftrightarrow} = 0.91\,\text{km}$. Thus, for clouds with a prevailing directional structure

11

it is advisable to give variable ξ_τ as a function of observation direction, e.g., by two parameters, $\xi_\tau^{\updownarrow}$ along and $\xi_\tau^{\leftrightarrow}$ across the prevailing cloud structure.
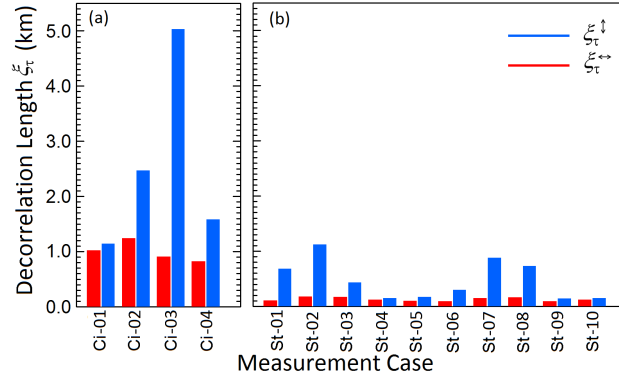
<mark>The decorrelation lengths are calculated for each measurement case along ($\bar{\xi}_\tau^{\updownarrow}$) and across ($\bar{\xi}_\tau^{\leftrightarrow}$) the prevailing directional structure of the cloud inhomogeneities, which is identified by the 2D autocorrelation analysis.</mark> Table 2 summarizes and Fig. 4 illustrates the resulting $\bar{\xi}_\tau^{\updownarrow}$ (blue bars) and $\bar{\xi}_\tau^{\leftrightarrow}$ (red bars). Additionally, $\bar{\xi}_\tau \pm \sigma_\xi$ are included ($\bar{\xi}_\tau^{\updownarrow} \pm \sigma_\xi$, $\bar{\xi}_\tau^{\leftrightarrow} \pm \sigma_\xi$) in Tab. 2. Those values illustrate the pixel-by-pixel variability for the calculated $P_\tau^2(L_x, L_y)$ along one direction. Due to the exponential behaviour of $P_\tau^2(L_x, L_y)$ they are asymmetric with respect to $\bar{\xi}_\tau^{\updownarrow}$ and $\bar{\xi}_\tau^{\leftrightarrow}$.

Table 2. Decorrelation length calculated for the retrieved fields of τ from the CARRIBA (Ci-01–Ci-04) and VERDI (St-01–St-10) campaigns. Vertical arrows ($\updownarrow$) indicate the calculation of $P_\tau^2(L_x, L_y)$ and subsequent derivation of ξ_τ along L_y, horizontal arrows ($\leftrightarrow$) along L_x. Furthermore, $\bar{\xi}_\tau$ is the average of all pixels, $\bar{\xi}_\tau - \sigma_\xi$ is the average minus standard deviation, and $\bar{\xi}_\tau + \sigma_\xi$ is the average plus standard deviation.

Case	$\bar{\xi}_\tau^{\updownarrow} - \sigma_\xi$ (km)	$\bar{\xi}_\tau^{\updownarrow}$ (km)	$\bar{\xi}_\tau^{\updownarrow} + \sigma_\xi$ (km)	$\bar{\xi}_\tau^{\leftrightarrow} - \sigma_\xi$ (km)	$\bar{\xi}_\tau^{\leftrightarrow}$ (km)	$\bar{\xi}_\tau^{\leftrightarrow} + \sigma_\xi$ (km)
Ci-01	0.72	1.14	1.62	0.62	1.02	1.48
Ci-02	2.16	2.47	3.42	1.12	1.24	1.39
Ci-03	4.42	5.03	6.34	0.62	0.91	1.41
Ci-04	1.20	1.58	2.12	0.71	0.82	1.26
St-01	0.46	0.68	0.89	0.07	0.11	0.17
St-02	0.67	1.12	1.56	0.11	0.18	0.26
St-03	0.37	0.43	0.55	0.11	0.17	0.26
St-04	0.11	0.15	0.25	0.08	0.12	0.19
St-05	0.13	0.17	0.26	0.07	0.10	0.17
St-06	0.23	0.30	0.37	0.06	0.09	0.15
St-07	0.44	0.88	1.64	0.09	0.15	0.26
St-08	0.30	0.73	1.57	0.13	0.16	0.24
St-09	0.11	0.14	0.24	0.05	0.09	0.16
St-10	0.12	0.15	0.26	0.08	0.12	0.21

The results show that the observed subtropical cirrus yield larger decorrelation lengths $\bar{\xi}_\tau$ than the Arctic stratus cases. Thus, the subtropical cirrus cases are more homogeneous than the Arctic stratus cases. <mark>Furthermore, the results indicate that for most of the measurement cases a distinct directional structure of cloud inhomogeneities is observed. The results for $\bar{\xi}_\tau^{\updownarrow}$ are in 9 of the 14 investigated cases more than twice as large as for $\bar{\xi}_\tau^{\leftrightarrow}$.</mark>

For the subtropical cirrus, ξ_τ varies from 0.82 km to 5.03 km, depending on the cloud structure and inhomogeneity. The rather inhomogeneous cases Ci-01 and Ci-04 with highly variable τ_{ci} on small scales yield rapidly decreasing $P_\tau^2(L_x, L_y)$ with low $\bar{\xi}_\tau$. In contrast, the quite homogeneous

Figure 4. Decorrelation length calculated for the retrieved fields of τ from the **(a)** CARRIBA (Ci-01–Ci-04) and **(b)** VERDI (St-01–St-10) campaigns. Vertical arrows ($\updownarrow$) indicate the calculation of $P_\tau^2(L_\mathrm{x}, L_\mathrm{y})$ and subsequent derivation of ξ_τ along L_y, horizontal arrows ($\leftrightarrow$) along L_x.

cases Ci-02 and Ci-03 yield slowly decreasing $P_\tau^2(L_\mathrm{x}, L_\mathrm{y})$ and larger $\bar{\xi}_\tau$. The differences between $\bar{\xi}_\tau^{\updownarrow}$ and $\bar{\xi}_\tau^{\leftrightarrow}$ reach up to 82 %.

For the Arctic stratus fields observed during VERDI, $\bar{\xi}_\tau^{\updownarrow}$ and $\bar{\xi}_\tau^{\leftrightarrow}$ range between 0.09 km and
295   1.12 km. Similar to the CARRIBA cirrus cases, the differences between $\bar{\xi}_\tau^{\updownarrow}$ and $\bar{\xi}_\tau^{\leftrightarrow}$ are significant reaching values of up to 84 %.

However, the absolute values of $\bar{\xi}_\tau^{\updownarrow}$ and $\bar{\xi}_\tau^{\leftrightarrow}$ for the Arctic stratus are smaller (more inhomogeneous) than those for the subtropical cirrus, although the 1D inhomogeneity parameters from Tab. 1 yield similar values. This reveals that the 1D inhomogeneity parameters ρ_τ, S_τ, and χ_τ just provide
300   incomplete information for a comparison of different types of clouds as they are not able to consider the horizontal structure of cloud inhomogeneities. Differences can only be observed by an evaluation of the horizontal pattern of the cloud inhomogeneities.

5   Power Spectral Density Analysis

Multiple scattering in inhomogeneous 3D cloud structures causes a smoothing of the reflected ra-
305   diances I_λ above clouds (Cahalan and Snider, 1989; Marshak et al., 1995). This effect generates uncertainties in the retrieved fields of τ if homogeneous plane-parallel clouds are assumed in the retrieval. Therefore, in this paper the smoothing effect is analyzed using the Fourier transform of the retrieved fields of τ. The application of Fourier transforms for the investigation of cloud inhomogeneities is widely used in the existing literature (e.g., Cahalan, 1994; Davis et al., 1999a; Schröder,
310   2004). However, in most of these studies, the 1D Fourier transformation is adopted to narrow pixel-lines of radiative quantities such as I_λ or the reflectivity γ_λ. Here, a 2D Fourier transformation is applied to spatial 2D cloud scenes. Schäfer et al. (2013) showed that angular features of the scatter-

13

ing phase functions are imprinted in the I_λ measurements of AisaEAGLE. To avoid artifacts in the Fourier transform arising from those features, fields of τ are used for the analysis.

315   The Fourier transformation decomposes a periodic function into a sum of sinusoidal base functions. For a given measurement, here $\tau(x, y)$, the 2D Fourier transform $\mathcal{F}_\tau(k_x, k_y)$ is defined by:

$$\mathcal{F}_\tau(k_x, k_y) = \int\limits_{-\infty}^{\infty} \int\limits_{-\infty}^{\infty} \tau(x, y) \cdot e^{-2\pi i \cdot (k_x x + k_y y)} \, \mathrm{d}x \, \mathrm{d}y, \tag{6}$$

The base functions are described by a complex exponential of different frequency. The fields of τ are
320   given as a function of horizontal distances x and y. Therefore, wave numbers $k_x = 1/x$ and $k_y = 1/y$ are used in the base functions.

The Fourier coefficients $\mathcal{F}_\tau(k_x, k_y)$ are calculated using a Discrete Fourier Transform (DFT). With n and m discrete elements in the x_j and y_k dimension of the τ field, the 2D DFT is derived by:

$$\mathrm{DFT}(k_x, k_y) = \frac{1}{n \cdot m} \sum_{x_j=0}^{n-1} \sum_{y_k=0}^{m-1} \tau(x_j, y_k) \cdot e^{-2\pi i \cdot \left(\frac{k_x x_j}{n} + \frac{k_y y_k}{m} \right)}. \tag{7}$$

325   Figures 5 and 6 present the Fourier transform in the form of power spectral densities $E(k_x)$ and $E(k_y)$, in the following called $E(k_x, k_y)$, calculated from the complex Fourier coefficients by:

$$E(k_x, k_y) = \mathrm{DFT}^2(k_x, k_y). \tag{8}$$

Figures 5a to 5c show τ_{ci} fields of three selected cloud areas of 3.5 km by 3.5 km size extracted from the cases Ci-01, Ci-02, and Ci-03. Ci-01 represents an inhomogeneous subtropical cirrus with-
330   out a preferred direction in the cloud structure (Fig. 5a). In Ci-02 a homogeneous subtropical cirrus with a moderate directional structure (Fig. 5b) is selected, while in Ci-03 an inhomogeneous subtropical cirrus with a distinct directional structure (Fig. 5c) is presented. Figures 5d to 5f show the corresponding logarithm of the 2D power spectral densities $E(k_x, k_y)$. Largest values of $E(k_x, k_y)$ are found at smallest wave numbers k_x and k_y, which are located in the center of the image. In gen-
335   eral the values of $E(k_x, k_y)$ decrease with increasing k_x and k_y. Inhomogeneous clouds (Figs. 5d and 5f) show higher values of $E(k_x, k_y)$ over a wide range of wave numbers k_x and k_y, whereas the dominating $E(k_x, k_y)$ for homogeneous clouds (Fig. 5e) are only located close to the smallest wave numbers k_x and k_y. Similar to the autocorrelation functions the decrease of $E(k_x, k_y)$ is rotationally symmetric for clouds with no preferred directional structure (Fig. 5d), but asymmetrical for clouds
340   with a prevailing directional structure (Figs. 5e, 5f).

To quantify the two-dimensional nature of the symmetry, Figs. 5g to 5f show the $E(k_x, k_y)$ along (black, E_b) and across (red, E_a) the direction of the strongest symmetry axis. For the inhomogeneous case without a prevailing directional structure (Ci-01), both components E_a and E_b are almost identical. For the homogeneous case with a moderate directional structure (Ci-02), both E_a and
345   E_b are similar over most of the covered range of k_x and k_y, except for the smallest wave number
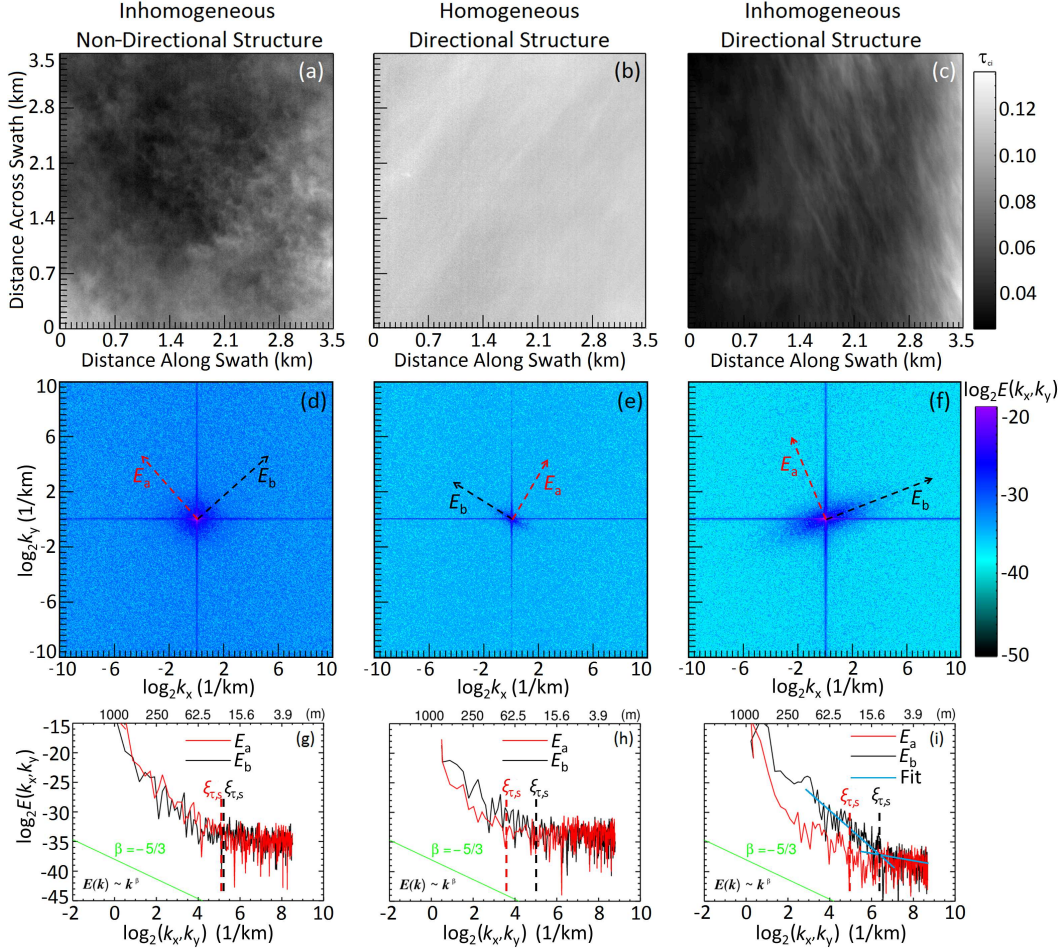
Figure 5. (a-c) AisaEAGLE image (3.5 by 3.5 km), **(d-f)** 2D power spectral density $E(k_x, k_y)$, and **(g-i)** 1D power spectral density $E(k_x, k_y)$ across (red arrows, E_a) and along (black arrows, E_b) the prevailing direction of scale invariant areas for **(a)**, **(d)**, **(g)** inhomogeneous cloud without directional structure, **(b)**, **(e)**, **(h)** homogeneous cloud with slight directional structure, and **(c)**, **(f)**, **(i)** inhomogeneous cloud with distinct directional structure. The $\xi_{\tau,s}$ are marked by colored dashed lines.

$k_x < 3\,\mathrm{km}^{-1}$ and $k_y < 3\,\mathrm{km}^{-1}$. For the inhomogeneous case with a distinct directional structure (Ci-03), both E_a and E_b are of similar magnitude only at $k_x > 7\,\mathrm{km}^{-1}$ and $k_y > 7\,\mathrm{km}^{-1}$. The differences in E_a and E_b of clouds with a prevailing directional structure result from the different k_x and k_y, at which the signal turns into white noise (constant $E(k_x, k_y)$, independent of k_x and k_y).

350 This transition is used to characterize the small-scale break $\xi_{\tau,s}$, which determines the lower size range of the detected cloud inhomogeneities and identifies the scale at which the measurements turn into white noise. To derive $\xi_{\tau,s}$, fits are applied to the two scale-invariant regimes of $E(k_x, k_y)$ (shown for E_b in Fig. 5i). Subsequently, the small scale break $\xi_{\tau,s}$ is determined as the intersection of those fits. The small scale break $\xi_{\tau,s}$ is connected to the pixel size, which depends on the distance be-

15

355 tween cloud and sensor. The corresponding k_x and k_y give $\xi_{\tau,s}$. The small-scale breaks $\xi_{\tau,s}(E_a)$ and $\xi_{\tau,s}(E_b)$ for case Ci-01 are at about 0.03 km ($\log_2 k_{x,y} \approx 5$). For Case Ci-02, $\xi_{\tau,s}(E_a)$ and $\xi_{\tau,s}(E_b)$ are in the length range of 0.09 km ($\log_2 k_{x,y} \approx 3.5$) and 0.03 km ($\log_2 k_{x,y} \approx 5$), respectively. The small-scale break $\xi_{\tau,s}(E_a)$ from case Ci-03 is at about 0.03 km ($\log_2 k_{x,y} \approx 5$), while $\xi_{\tau,s}(E_b)$ is at about 0.01 km ($\log_2 k_{x,y} \approx 6.5$), which is already close to the pixel size, which corresponds to the

360 lower detection limit that leads to white noise. Thus, $\xi_{\tau,s}$ yields quantitatively larger values along the prevailing cloud structure than across. Furthermore, the ranges of the derived small-scale breaks $\xi_{\tau,s}$ are found to be close to the ranges of the small-scale breaks reported in literature. Davis et al. (1999b) derived small-scale breaks for a broken-stratocumulus/towering cumulus cloud complex from LWC measurements with a particulate volume monitor probe (4 cm resolution) at ranges of

365 about 2-5 m. They proposed that those small-scale breaks are related to extreme values in the detected LWC, which appear on small horizontal scales. Besides Poissonian fluctuations of the cloud optical thickness τ and the white noise related to power spectral signals at scales below the pixel size this might be a further explanation for the derived small-scale breaks in the current study and needs to be investigated in further studies.

370 Marshak et al. (1995) discussed that cloud inhomogeneity and horizontal photon transport are scale–dependent processes. The $E(k_x, k_y)$ of cloud optical and microphysical properties are proportional to k_x^β and k_y^β, where β is the slope of the power spectral density. At large scales, the $E(k_x, k_y)$ of e.g. I_λ, τ, LWC, or IWC follow Kolmogorov's $\beta = -5/3$ law of energy distribution in a turbulent fluid (Kolmogorov, 1941). At these scales, the variability in the radiation field follows the variabil-

375 ity in LWC. Increasing cloud inhomogeneity causes a decrease of β of optical properties at smaller scales, but not in β of microphysical properties. At scales influenced by horizontal photon transport, β may differ from -5/3 dependent on the cloud inhomogeneity that changes the magnitude of horizontal photon transport. Typically, this affects horizontal scales smaller than 1000 m. The higher the cloud inhomogeneity, the larger the deviation from -5/3. Thus the slope β at scales below 1000 m

380 provides a measure of cloud inhomogeneity. Usually, the scale break ξ is used to quantify the deviation from -5/3. In the following, the horizontal scale at which the power spectrum starts to deviate from the -5/3 law defines the large-scale break $\xi_{\tau,L}$. The position of the large-scale break depends on the size of the horizontal cloud structures; more inhomogeneous clouds with larger variability on smaller scales yield smaller $\xi_{\tau,L}$. For scales smaller than $\xi_{\tau,L}$, the radiative smoothing leads to

385 uncertainties in 1D cloud retrievals, where the horizontal photon transport is automatically neglected (Cahalan, 1994; Marshak et al., 1998; Zinner et al., 2006; Varnai and Marshak, 2007).

A comparison of the $E(k_x, k_y)$ to the -5/3 law in Figs. 5g to 5h shows that the analyzed scenes are too small to cover the larger scales, which are necessary to identify $\xi_{\tau,L}$. The range of k_x and k_y is lower than $\xi_{\tau,L}$ and $E(k_x, k_y)$ already exhibit a steeper slope than $\beta = -5/3$. Therefore, the size

390 of the selected areas was extended. Unfortunately, this is only possible for calculations of the DFT along L_y (across swath). Calculations along L_x (swath) do not cover a sufficiently large distance

to derive quantitative values for $\xi_{\tau,\mathrm{L}}$. Therefore, the following analysis is performed using 1D DFT along L_y only. Furthermore, both cloud cases, subtropical cirrus and Arctic stratus, exhibit a similar pixel length along L_y ($5\pm2\,\mathrm{m}$), which results from the chosen frame rate (subtropical cirrus: 4 Hz, Arctic stratus: 30 Hz) and given cloud ($\approx 20\,\mathrm{m\,s^{-1}}$) and aircraft ($\approx 70\,\mathrm{m\,s^{-1}}$) velocity. This allows a direct comparison between these two different cloud types with different observation geometry.

Figures 6a and 6b show the 1D DFT calculated across the swath for two typical cases of subtropical cirrus (CARRIBA case Ci-01) and Arctic stratus (VERDI case St-07). The two cases are selected, since they exhibit a similar length L_y. For each line of the τ field (each swath pixel) $E(k_\mathrm{y})$ is calculated and the individual power spectra are overlaid as gray dots in Fig.6. To evaluate the resulting 1D Fourier spectra with reduced noise (rn) characteristics, the $E_\mathrm{rn}(k) \sim k^{\beta}$ are calculated with the use of octave binning, following the method proposed by Davis et al. (1996), Harris et al. (1997), and Schröder (2004). Logarithmically spaced bins k_n are calculated by:

$$k_n = \frac{1}{2^n} \sum_{i=2n}^{2^{n+1}-1} k_i, n = 1, 2, ..., \log_2(N-2), \tag{9}$$

for the number of data points N. $E(k_\mathrm{rn})$ is then obtained by:

$$E(k_\mathrm{rn}) = \frac{1}{2^n} \sum_{i=2n}^{2^{n+1}-1} E(k_i), n = 1, 2, ..., \log_2(N-2). \tag{10}$$

Within each bin 2^n data points are averaged. In addition to the reduced noise of $E(k_\mathrm{rn})$ compared to $E(k_\mathrm{y})$ the binning provides a uniform contribution of all scales to the average values.

The $E(k_\mathrm{rn})$ derived from the octave binning are included as green diamonds in Fig.6. The data of the octave binning were used to fit the spectra for different slopes in the different scale ranges. A green line indicates the $\beta = -5/3$ law. For large scales, the $E_\mathrm{rn}(k_\mathrm{y})$ (blue fit) approximately follow the $-5/3$ relation in both cases. The large-scale break ($\xi_{\tau,\mathrm{L}}$) is evident at the intersection between the blue and the red line. Here, the slope in the $E_\mathrm{rn}(k_\mathrm{y})$ becomes steeper. For the CARRIBA case $\xi_{\tau,\mathrm{L}} = 0.31\,\mathrm{km}$ and the middle scale slope β_m decreases to -2.2. For the VERDI case $\xi_{\tau,\mathrm{L}} = 0.06\,\mathrm{km}$ and β_m decreases to -2.2. The middle–scale slope β_m is a function of the inhomogeneity in the measured signals. With increasing inhomogeneity of the optical thickness τ, β_m decreases. Together with the smaller $\xi_{\tau,\mathrm{L}}$, this indicates that the selected Arctic stratus case is more inhomogeneous compared to the selected subtropical cirrus case. As discussed above, $\xi_{\tau,\mathrm{s}}$ is observed at the intersection between the fits for the middle (red, β_m) and small scales (orange, β_s). Due to the analysis of a significant larger distance compared to Fig. 5, it is highly uncertain to give quantitative numbers for $\xi_{\tau,\mathrm{s}}$. Therefore, it is indicated only qualitatively. However, $\xi_{\tau,\mathrm{s}}$ identifies at which scales the measurements turn into noise. The scale depends on the distance between sensor and cloud. For the sensor, noise dominated at scales two times pixel range, which corresponds to about 15 m for the subtropical cirrus observations ($\approx 12\,\mathrm{km}$ cloud base altitude) and 3.5 m for the Arctic stratus observations where the aircraft was closer to cloud top ($\approx 2\,\mathrm{km}$ distance).
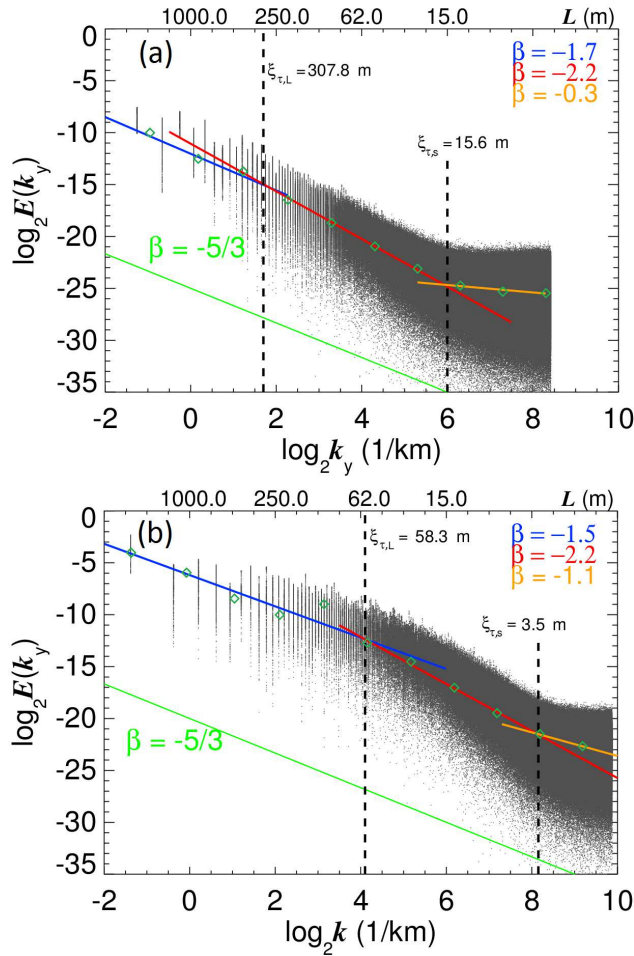
Figure 6. 1D power spectral density $E(k_y)$ (gray dots) for each spatial pixel on the swath axis of the τ field from **(a)** case Ci-01 and **(b)** case St-07. Scale-invariant slopes β are marked with colored solid lines. The $E(k_{rn})$ derived from the octave binning are included as dark green diamonds. Scale breaks $\xi_{\tau,L}$ and $\xi_{\tau,s}$ are indicated by dashed lines.

Figure 7 illustrates $\xi_{\tau,L}$ for all available cloud cases from CARRIBA and VERDI. ==Especially the values for the Arctic stratus are in the size range, which was also reported by Marshak et al. (1995), who found scale breaks for fractal clouds in the range of 200–500 m.== Furthermore, the values compare well with the derived decorrelation length ξ_τ derived in Sect. 4. Although the exact values

430 of $\xi_{\tau,L}$ are not equal to ξ_τ, both are in the same size range for each individual case. Similar to ξ_τ given in Tab. 2, $\xi_{\tau,L}$ confirms that Ci-02 and Ci-03 are more homogeneous than Ci-01 and Ci-04. ==Furthermore, the resulting large scale breaks $\xi_{\tau,L}$ confirm the results from the derived decorrelation lengths ξ_τ that the subtropical cirrus observed during CARRIBA is more homogeneous (larger ξ_τ and $\xi_{\tau,L}$) than the Arctic stratus from VERDI (smaller ξ_τ and $\xi_{\tau,L}$). This is related to the fact that==

18
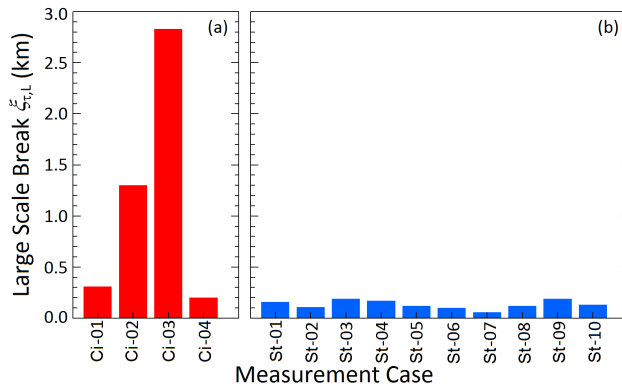
Figure 7. Across swath derived large scale breaks $\xi_{\tau,\mathrm{L}}$ for the retrieved fields of τ from the **(a)** CARRIBA (Ci-01 to Ci-04, red) and **(b)** VERDI (St-01 to St-10, blue) campaigns. The values were derived by using the method presented in Fig. 6.

435 $\xi_{\tau,\mathrm{L}}$, which is the radiative smoothing scale, is a function of the cloud geometrical thickness and the transport mean free path. For Arctic stratus both parameters are significantly smaller than for subtropical cirrus."

An estimation of the uncertainty in the derived $\xi_{\tau,\mathrm{L}}$ can be obtained from a comparison to investigations performed by Schröder and Bennartz (2003). Amongst others, Schröder and Bennartz (2003)

440 investigated scale breaks as a function of wavelengths and absorption bands. Their results show uncertainties in a range of 3 % to 8 %. Schröder and Bennartz (2003) derived those uncertainty values by subsetting the points of the power spectrum that are used for the slope fit. Using this method, they obtained a set of different slopes and scale breaks. The particular standard deviations of those sets are used as an uncertainty for the octave binning method. Applied to the VERDI cases, the 3 %

445 to 8 % result in a maximum uncertainty of $\pm\,5\,\mathrm{m}$ (St-07) to $\pm\,15\,\mathrm{m}$ (St-03, St-09) in the derived $\xi_{\tau,\mathrm{L}}$. For the CARRIBA cases the maximum uncertainty is in the range of 16 (Ci-04) to 226 m (Ci-03). However, especially case Ci-03 is characterized as rather homogeneous. Therefore, much lower uncertainty values are to be expected.

6 Summary and Conclusions

450 During the two field campaigns CARRIBA and VERDI, downward (ground-based) and upward (measured from aircraft) fields of solar spectral radiance ($I_\lambda^\downarrow$, $I_\lambda^\uparrow$) were measured with high spatial resolution (less than $10\,\mathrm{m}$), using the imaging spectrometer AisaEAGLE. The measured radiance fields were used to retrieve fields of τ, which were subsequently analyzed to quantify horizontal cloud inhomogeneities. Furthermore, due to the observation of 2D fields, the prevailing directional

455 structure of the cloud inhomogeneities was investigated.

19

Four subtropical cirrus cases collected during CARRIBA and ten Arctic stratus cases sampled during VERDI were studied in detail. The cloud inhomogeneity was quantified by three 1D inhomogeneity parameters ρ_τ, S_τ, and χ_τ, as well as 1D and 2D autocorrelation functions, and Fourier analysis.

460   Considering the pixel and domain size of the analyzed measurements, the results from the calculated 1D inhomogeneity parameters ρ_τ and S_τ are in agreement with values given in the literature for similar cloud types. The calculated ρ_τ are in the range of 0.17–0.91 for the subtropical cirrus observed during CARRIBA and 0.15–0.34 for the Arctic stratus measured during VERDI. The literature values are in the range of 0.07–0.78. The inhomogeneity parameter S_τ exhibits values of

465   0.08 to 0.48 for CARRIBA and 0.07 to 0.20 for VERDI, which agrees with values of 0.03 to 0.3 given in literature. For χ_τ, the literature estimates values between ≈ 0.65 and 0.8, while the results from CARRIBA and VERDI are significantly larger. This is probably related to the different pixel and domain sizes. All values except for Ci-04 ($\chi_\tau = 0.63$) are in the range between 0.92 and 0.99. A further comparison between the results for the clouds encountered during CARRIBA and

470   VERDI showed that all three 1D inhomogeneity parameters exhibit values of similar magnitude for both cloud types; subtropical cirrus and Arctic stratus. This might lead to the conclusion that the inhomogeneity of both cloud types could be treated by the same 1D inhomogeneity parameters.

    However, the comparison of the 2D analysis of squared autocorrelation functions $P_\tau^2(L_x, L_y)$ with the 1D inhomogeneity parameters ρ_τ, S_τ, and χ_τ showed that it is important to consider the full

475   horizontal structure of clouds using 2D analysis rather than 1D analysis, when determining cloud inhomogeneity. For both cloud cases (subtropical cirrus, Arctic stratus) the 1D inhomogeneity parameters yield similar values, but significant differences resulting from the analysis of $P_\tau^2(L_x, L_y)$, which additionally contain information about the horizontal structure of cloud inhomogeneities. The 1D inhomogeneity parameters are not capable of differentiating the directional structure of clouds

480   and may lead to misinterpretations of cloud inhomogeneity. From the squared autocorrelation functions $P_\tau^2(L_x, L_y)$ the decorrelation length ξ_τ was derived, which is a measure of the size range of the cloud inhomogeneities. The 2D analysis of $P_\tau^2(L_x, L_y)$ revealed that ξ_τ is a function of the directional structure of the cloud inhomogeneities. Without knowledge of the directional structure of cloud inhomogeneities, no universally valid value for ξ_τ can be derived from the retrieved fields of

485   τ. The differences in ξ_τ as derived from a 1D autocorrelation analysis along and across the prevailing structure of cloud inhomogeneities reached up to 82 % and 84 % for CARRIBA and VERDI, respectively. It is concluded that the directional cloud structure has to be taken into account for a quantification of cloud inhomogeneities. The absolute values of ξ_τ were in the range of 0.82 km to 5.03 km for CARRIBA and 0.09 km to 1.12 km for VERDI. Furthermore, the results from the

490   2D analysis showed that for the observed cloud cases the subtropical cirrus was more homogeneous than the Arctic stratus. This result was not available from the investigation of the commonly used 1D inhomogeneity parameters. Therefore, using 2D methods in future studies for the characterization

20

of cloud inhomogeneities is advisable, since their information content exceeds the information content of the commonly used 1D inhomogeneity parameters. Nowadays, 2D images of cloud fields are widespread by e.g., measurements of all-sky cameras or satellite observation with high spatial resolution. Applying the presented methods to such continuous measurements would provide detailed views into the climatology of cloud inhomogeneities.

3D radiative effects are quantified by applying 2D Fourier transformation to the retrieved fields of τ. The power spectral densities $E(k_{x,y})$ calculated from the Fourier Transform of $I_\lambda^\downarrow$ and $I_\lambda^\uparrow$ show evidence that 3D radiative effects did affect the radiation field of both cloud types, subtropical cirrus and Arctic stratus. For larger scales ($> 1000\,\mathrm{m}$), no horizontal photon transport was observed as the $E(k_{x,y})$ followed Kolmogorov's -5/3 law. Approaching smaller scales ($< 1000\,\mathrm{m}$), the derived slopes become steeper indicating radiative smoothing by cloud inhomogeneities and horizontal photon transport. From the intersection of fits of the three slope regimes, the small-scale break $\xi_{\tau,s}$ (between small- and middle-scale slopes) and the large-scale break $\xi_{\tau,L}$ (between middle- and large-scale slopes) were derived. Similarly to the analysis using autocorrelation functions, $\xi_{\tau,s}$ depends on the directional structure of the cloud inhomogeneities. Due to a too small swath width, a similar analysis for $\xi_{\tau,L}$ could not be performed. However, the calculated $\xi_{\tau,L}$ along the image are comparable to the results derived from the analysis of $P_\tau(L_x, L_y)$. The large-scale break $\xi_{\tau,L}$ for CARRIBA was in the range of $0.20\,\mathrm{km}$ to $2.83\,\mathrm{km}$. For VERDI a range of $0.06\,\mathrm{km}$ to $0.19\,\mathrm{km}$ was covered by $\xi_{\tau,L}$.

In early studies, by e.g. Marshak et al. (1998) or Schröder (2004), the scale dependence of cloud radiation measurements was analyzed along one direction (narrow pixel-lines) using 1D DFT. However, the resulting $E(k)$ are valid for the particular observation direction along the given path only. Due to prevailing wind directions, clouds tend to evolve directional structures. In such cases, the calculated $E(k)$, β, $\xi_{\tau,s}$, and $\xi_{\tau,L}$ will only be valid for the whole cloud if the cloud structure exhibits a non-directional character (compare Figs. 2b and 3a). In all other cases, significant differences can be expected (compare Figs. 2d and 3b). We found such differences for more than the half of the observed cloud scenes. Therefore, the directional structure of cloud inhomogeneities should be taken into account, when cloud inhomogeneities are characterized. It is expected that the information content derived from the directional analysis of cloud inhomogeneities can clearly improve sub-grid scale parametrizations in weather and climate models. For this, depending on the application, the decorrelation length (size and structure of cloud inhomogeneities) or the scale breaks (horizontal photon transport, 3D radiative effects) may provide better proxies compared to commonly used 1D inhomogeneity parameters.

However, so far only two cloud types were investigated. To build up a better idea on cloud inhomogeneity of different cloud types, more high definition observations of cloud fields are needed. Beside dedicated field campaigns, continuous observations by all-sky cameras or satellites with high

spatial resolution such as LandSat (15-90 m resolution) or ASTER (Advanced Spaceborne Thermal Emission and Reflection Radiometer, 15-90 m resolution) may provide the required data.

The 1D and 2D autocorrelation functions and Fourier analysis in conjunction with the derived decorrelation length and scale break are a helpful tool to verify cloud resolving models in terms of typical horizontal cloud geometries.

22

References

545 Albrecht, B. A.: Aerosols, Cloud Microphysics, and Fractional Cloudiness, Science, 245, 1227–1230, http://www.sciencemag.org/content/245/4923/1227.abstract, 1989.

Barker, H., Wielicki, B., and Parker, L.: A parameterization for computing grid-averaged solar fluxes for inhomogeneous marine boundary layer clouds. Part II: Validation using satellite data, J. Atmos. Sci., 53, 2304–2316, 1996.

550 Barlakas, V., Macke, A., and Wendisch, M.: SPARTA - Solver for Polarized Atmospheric Radiative Transfer Applications: Introduction and application in Saharan dust fields, J. Quant. Spectr. & Rad. Trans., doi:10.1016/j.jqsrt.2016.02.019, http://dx.doi.org/10.1016/j.jqsrt.2016.02.019, 2016.

Bierwirth, E., Ehrlich, A., Wendisch, M., Gayet, J.-F., Gourbeyre, C., Dupuy, R., Herber, A., Neuber, R., and Lampert, A.: Optical thickness and effective radius of Arctic boundary-layer clouds retrieved from airborne
555 nadir and imaging spectrometry, Atmos. Meas. Tech., 6, 1189–1200, doi:10.5194/amt-6-1189-2013, 2013.

Cahalan, R.: Bounded cascade clouds: albedo and effective thickness, Nonlin. Proc. Geophys., 1, 1994.

Cahalan, R. and Snider, J.: Marine stratocumulus structure, Remote Sens. Environ., 28, 95–107, 1989.

Carlin, B., Fu, Q., Lohmann, U., Mace, G., Sassen, K., and Comstock, J.: High-cloud horizontal inhomogeneity and solar albedo bias, J. Climate, 15, 2321–2339, 2002.

560 Choi, Y.-S. and Ho, C.-H.: Radiative effect of cirrus with different optical properties over the tropics in MODIS and CERES observations, Geophys. Res. Lett., 33, doi:10.1029/2006GL027 403, 2006.

Davis, A., Marshak, A., Wiscombe, W., and Cahalan, R.: Scale invariance in liquid water distributions in marine stratocumulus. Part I: Spectral properties and stationarity issues, J. Atmos. Sci., 53, 1538–1558, 1996.

Davis, A., Cahalan, R., Spinhirne, D., McGill, M., and Love, S.: Off-beam Lidar: an emerging technique in
565 cloud remote sensing based on radiative Green-function theory in the diffusion domain, Phys. Chem. Earth (B), 24, 177–185, 1999a.

Davis, A., Marshak, A., Gerber, H., and Wiscombe, W.: Horizontal structure of marine boundary layer clouds from centimeter to kilometer scales, J. Geophys. Res., 104, 6123–6144, 1999b.

Francis, P., Hignett, P., and Macke, A.: The retrieval of cirrus cloud properties from aircraft multi-spectral
570 reflectance measurements during EUCREX '93, Quart. J. Roy. Meteor. Soc., 124, 1273–1291, 1998.

Garrett, T. J., Gerber, H., Baumgardner, D. G., Twohy, C. H., and Weinstock, E. M.: Small, highly reflective ice crystals in low-latitude cirrus, Geophys. Res. Lett., 30, doi:10.1029/2003GL018 153, 2003.

Hanus, J., Malenovsky, Z., Homolova, L., Veroslav, K., Petr, L., and Pavel, C.: Potential of the VNIR Airborne hyperspectral system AISA Eagle, in: Symposium GIS Ostrava, (CZ), 2008.

575 Harris, D., Seed, A., Menabde, M., and Austin, G.: Factors affecting multiscaling analysis of rainfall time series, Nonlin. Proc. Geophys., 4, 137–156, 1997.

Hill, P. G., Hogan, R. J., Manners, J., and Petch, J. C.: Parametrizing the horizontal inhomogeneity of ice water content using CloudSat data products, Q. J. R. Meteorol. Soc., 138, 1784–1793, 2012.

Huang, D. and Liu, Y.: A novel approach for introducing cloud spatial structure into cloud radiative transfer
580 parameterizations, Environ. Res. Lett., 9, 124 022, 2014.

IPCC: Climate Change 2013: The Physical Science Basis, Cambridge University Press, 2013.

Iwabuchi, H.: Effects of cloud horizontal inhomogeneity on optical remote sensing of cloud parameters, Ph.D. thesis, Center for Atmospheric and Oceanic Studies, Graduate School of Science, Tokohu University, 2000.

23

Iwabuchi, H. and Hayasaka, T.: Effects of cloud horizontal inhomogeneity on the optical thickness
retrieved from moderate-resolution satellite data, J. Atmos. Sci., 59, 2227–2242, doi:10.1175/1520-
0469(2002)059<2227:EOCHIO>2.0.CO;2, 2002.

Kolmogorov, A.: Die Energiedissipation für lokalisotrope Turbulenz, Dokl. Akad. Nauk SSSR, 32, 16–18,
Nachdruck in: H. Goering Hrsg., 1958: Statistische Theorie der Turbulenz., Akademie–Verlag, Berlin, 71–
76., 1941.

Loeb, N. and Davies, R.: Observational evidence of plane parallel model biases: Apparent dependence of cloud
optical depth on solar zenith angle, J. Geophys. Res., 101, 1621–1634, doi:10.1029/95JD03298, 1996.

Loeb, N. G., Wielicki, B. A., Doelling, D. R., Smith, G. L., Keyes, D. F., Kato, S., Manalo-Smith, N., and
Wong, T.: Toward Optimal Closure of the Earth's Top-of-Atmosphere Radiation Budget, Journal of Climate,
22, 748–766, doi:10.1175/2008JCLI2637.1, 2009.

Marshak, A., Davis, A., Wiscombe, W., and Cahalan, R.: Radiative smoothing in fractal clouds, J. Geophys.
Res., 100, 26 247–26 261, 1995.

Marshak, A., Davis, A., Cahalan, R., and Wiscombe, W.: Nonlocal independent pixel approximation: Direct
and inverse problems, IEEE Trans. Geosci. Remote Sens., 36, 192–204, 1998.

Mayer, B. and Kylling, A.: Technical note: The *libRadtran* software package for radiative transfer calculations
- description and examples of use, Atmos. Chem. Phys., 5, 1855–1877, 2005.

Oreopoulos, L. and Cahalan, R. F.: Cloud Inhomogeneity from MODIS, J. Climate, 18, 5110–5124, 2005.

Oreopoulos, L., Cahalan, R., Marshak, A., and Wen, G.: A new normalized difference cloud retrieval technique
applied to Landsat radiances over the Oklahoma ARM site, J. Appl. Meteorol., 39, 2305–2321, 2000.

Pincus, R., Barker, H. W., and Morcrette, J. J.: A fast, flexible, approximate technique for computing radiative
transfer in inhomogeneous cloud fields, J. Geophys. Res., 108, 4376, doi:10.1029/2002JD003322, 2003.

Pinsky, M. and Khain, A.: Fine structure of cloud droplet concentration as seen from Fast-FSSP measurements.
Part II: Results of in-situ observations, J. Appl. Meteorol., 42, 65–73, 2003.

Rossow, W. and Schiffer, R.: Advances in understanding clouds from ISCCP, Bull. Amer. Meteorol. Soc., 80,
2261–2287, 1999.

Rozwadowska, A. and Cahalan, R. F.: Plane-parallel biases computed from inhomogeneous Arctic clouds and
sea ice, J. Geophys. Res., 107, 4384, 2002.

Schäfer, M., Bierwirth, E., Ehrlich, A., Heyner, F., and Wendisch, M.: Retrieval of cirrus optical thickness and
assessment of ice crystal shape from ground-based imaging spectrometry, Atmos. Meas. Tech., 6, 1855–
1868, doi:10.5194/amt-6-1855-2013, 2013.

Schäfer, M., Bierwirth, E., Ehrlich, A., Jäkel, E., and Wendisch, M.: Observations and simulations of three-
dimensional radiative interactions between Arctic boundary layer clouds and ice floes, Atmos. Chem. Phys.
Discuss., 15, 1421–1469, doi:10.5194/acpd-15-1421-2015, 2015.

Schröder, M.: Multiple scattering and absorption of solar radiation in the presence of three-dimensional cloud
fields, Ph.D. thesis, Fachbereich Geowissenschaften der Freien Universität Berlin, 2004.

Schröder, M. and Bennartz, R.: Impact of gas absorption and surface albedo on cloud radiative smooth-
ing, Geophysical Research Letters, 30, 1168–1171, doi:10.1029/2002GL016523, http://dx.doi.org/10.1029/
2002GL016523, 2003.

Shonk, J. K. P., Hogan, R. J., and Manners, J.: Impact of improved representation of horizontal and vertical cloud structure in a climate model, J. Clim., 38, 2365–2376, doi:10.1007/s00382-011-1174-2, 2011.

625 Siebert, H., Bethke, J., Bierwirth, E., Conrath, T., Dieckmann, K., Ditas, F., Ehrlich, A., Farrell, D., Hartmann, S., Izaguirre, M. A., Katzwinkel, J., Nuijens, L., Roberts, G., Schäfer, M., Shaw, R. A., Schmeissner, T., Serikov, I., Stevens, B., Stratmann, F., Wehner, B., Wendisch, M., Werner, F., and Wex, H.: The fine–scale structure of the trade wind cumuli over Barbados – an introduction to the CARRIBA project, Atmos. Chem. Phys., 13, 10 061–10 077, doi:doi:10.5194/acp-13-10061-2013, 2013.

630 Slingo, A.: Sensitivity of the Earth's Radiation Budget to Changes in Low Clouds, Nature, 343, 49–51, 1990.

Stephens, G.: Cloud feedbacks in the climate system: A critical review, J. Climate, 18, 237–273, 2005.

Stocker, T. F., Qin, D., Plattner, G. K., Tignor, M., Allen, S. K., Boschung, J., Nauels, A., Xia, Y., Bex, V., and Midgley, P. M., eds.: Climate Change 2013: The Physical Science Basis. Working Group I Contribution to the Fifth Assessment Report of the Intergovernmental Panel on Climate Change, Cambridge University

635 Press, UK, 2013.

Szczap, F., Isaka, H., Saute, M., and Guillemet, B.: Effective radiative properties of bounded cascade non-absorbing clouds: Definition of the equivalent homogeneous cloud approximation, J. Geophys. Res., 105, 20 617–20 633, 2000.

Varnai, T. and Marshak, A.: View angle dependence of cloud optical thicknesses retrieved by Moderate Reso-

640 lution Imaging Spectroradiometer (MODIS), J. Geophys. Res., 112, D06 203, doi:10.1029/2005JD006912, 2007.

Wendisch, M., Yang, P., and Ehrlich, A., eds.: Amplified climate changes in the Arctic: Role of clouds and atmospheric radiation, vol. 132, chap. 1, pp. 1–34, Sitzungsberichte der Sächsischen Akademie der Wissenschaften zu Leipzig, Mathematisch-Naturwissenschaftliche Klasse, S. Hirzel Verlag, 2013.

645 Zinner, T., Mannstein, H., and Tafferner, A.: Cb-TRAM: Tracking and monitoring severe convection from onset over rapid development to mature phase using multi-channel Meteosat-8 SEVIRI data, Meteorology and Applied Physics, submitted, 2006.

Zuidema, P. and Evans, K.: On the validity of the independent pixel approximation for boundary layer clouds observed during ASTEX, J. Geophys. Res., 103, 6059–6074, 1998.